AN ABSTRACT OF THE THESIS OF

Katharine Danielle Sarmast for the degree of Master of Science in Radiation Health Physics presented on November 19, 2010.

Title: MCNP5 Modeling of the Oregon State TRIGA® Reactor for SkyShine Dose Estimation After a Loss of Coolant Accident

Abstract approved:

Steve R. Reese

This thesis evaluates dose rates from the TRIGA® reactor by comparing ion chamber measured exposure rates to exposure rates calculated from MCNP5 model data. The first step evaluates the energy distribution required to match ion chamber exposure rates from measurements taken at 1 foot increments above the reactor core. Next, the back calculated source activity is used to determine the exposure rates, at those same 1 ft increments above the core, in the event of a loss of coolant accident (LOCA). Then the energies deposited in simulated ion chambers, above the core are used to determine the dose rate to a person standing on top of the reactor bioshield after a LOCA. The dose rates that are calculated using the MCNP5 data were compared to calculations from the Oregon State TRIGA® Reactor (OSTR) Safety Analysis Report (SAR). The final step is to determine the maximum dose rate at the OSTR facility perimeter after a LOCA, due to skyshine.

The MCNP5 results showed that OSTR SAR overestimates dose rates at the top of the reactor bioshield. The discrepancy stems from the OSTR SAR using worst case scenario data, while this report uses less conservative, yet accurate, assumptions. The instantaneous dose rates on the reactor building exterior from photon skyshine peak at approximately 30 mrem per hour. The integrated activity resulted in a dose rate of approximately .005 mrem within the first hour after the reactor has shut down.

MCNP5 Modeling of the Oregon State TRIGA® Reactor for SkyShine Dose Estimation After a Loss of Coolant Accident

By

Katharine Danielle Sarmast

A THESIS

Submitted to

Oregon State University

in partial fulfillment of
the requirements for the
degree of

Master of Science

Presented November 19, 2010
Commencement June 2011

Master of Science thesis of Katharine Danielle Sarmast presented on November 19, 2010.

APPROVED:

Major Professor, Representing Radiation Health Physics

Head of the Department of Nuclear Engineering and Radiation Health Physics

Dean of the Graduate School

I understand that my thesis will become part of the permanent collection of Oregon State University libraries. My signature below authorizes release of my thesis to any reader upon request.

Katharine Danielle Sarmast, Author

ACKNOWLEDGEMENTS

I would like to express my tremendous gratitude to all faculty and staff in the Nuclear Engineering and Radiation Health Physics department at Oregon State University. A special thank you goes to Dr. Steve Reese, whose assistance and guidance enabled me to complete my thesis topic. His patience is endless, and for that I am forever grateful.

I would also like to thank my family: my father Dan, who has taught me most of life's lessons; my sister Patricia and her family, who have encouraged me to get out and try different things; many other family and friends who are endless in their love and support. You are all such an integral part of my success and I love you all!

Special thanks go to my supportive husband, Waqar. He supported my decision to continue my education by moving halfway across the country with me, allowing me to attend OSU as an on campus student. With his encouragement and love, I am moving forward into a promising and bright future.

TABLE OF CONTENTS

TABLE OF CONTENTS (Continued)

Page

LIST OF FIGURES

Figure Page

LIST OF FIGURES (Continued)

Figure Page

LIST OF TABLES

MCNP5 Modeling of the Oregon State TRIGA® Reactor for SkyShine Dose Estimation After a Loss of Coolant Accident

1. Introduction

1.1 Research Objective

The objective of this thesis is to estimate photon dose rates, attributable to skyshine, from the Oregon State University TRIGA® reactor (OSTR) generated during a LOCA. Maximum dose rates in and around the reactor facility are achieved when the primary reactor water is removed or drained. A LOCA would be a scenario where the dose to workers and the public would be maximized.

Dose to workers and the public must not exceed limits set by the NRC for licensed activities. Regulations in 10 CFR 20 dictate dose limits allowable for radiation workers and members of the public from licensed activities. The dose to the public at facility boundaries should be less than 100 mrem in a year or 2 mrem in any one hour [1]. Modeling the OSTR with MCNP5 allows dose rates to be estimated in the event of a LOCA and benchmarked against values calculated in the OSTR SAR. The research will show that the dose rates are likely less than previously determined in the OSTR SAR.

1.2 TRIGA® Reactors

The TRIGA® (Testing, Research, Isotope, General Atomics) reactor provides an invaluable tool for nuclear engineering and radiation health physics students to study and evaluate nuclear processes. The reactor is situated toward the western edge of the OSU campus in Corvallis, Oregon. The reactor is licensed by the Nuclear Regulatory Commission (NRC) to operate up to 1.1 MW, and contains low enriched uranium (LEU) fuel.

Nuclear reactor operation safety is an issue that arose before the very first nuclear reactor, the Chicago Pile, became critical on December 2nd, 1942 [2]. Since then, the need for scientists to have a tool to help understand a nuclear chain reaction and reactor control has increased considerably. Prior to the development of research

reactors training for operators and scientists was very theoretical, with rare chances for practical training. This need resulted in the development of a small, low power reactor "that is safe even in the hands of a young graduate student" [3] – the TRIGA® reactor.

A negative public perception of nuclear power, and radiation in general, requires the nuclear industry to be as faultless as possible in designs and operation. The inherent safety in the TRIGA® design removes some error associated with human intervention, and allows the reactor to power down in the event of mechanical system failure [4]. TRIGA® inherent safety is accomplished with a fuel design in which negative feedback occurs in the reactivity as temperature increases to safely shutdown the reactor.

1.2.1 TRIGA® Background

TRIGA® reactors were developed by General Atomics as one of their initiatives to create peaceful uses for nuclear technology. The original TRIGA® Mark I was designed with graphite reflected core located in an open tank of water which was all placed underground. The OSTR is a Mark II version. The Mark II is similar to the Mark I in design except the water tank and core sit above ground and is surrounded by a concrete bioshield.

The core of the reactor sits below approximately 16 feet of water. Surrounding the core is an 8 inch graphite reflector also containing 2 inches of lead. Approximately 12 inches of water is followed by approximately 8 feet of the cement bioshield. The core consists of 87 LEU Uranium/Zirconium hydride fuel elements and 4 control rods in a circular grid array. Each fuel element has graphite reflectors at each end, and is surrounded by stainless steel cladding. The reactor operates at 1.1 MW, and can pulse up to approximately 2,000 MW [5]. Figure 1 shows a side view of OSTR.

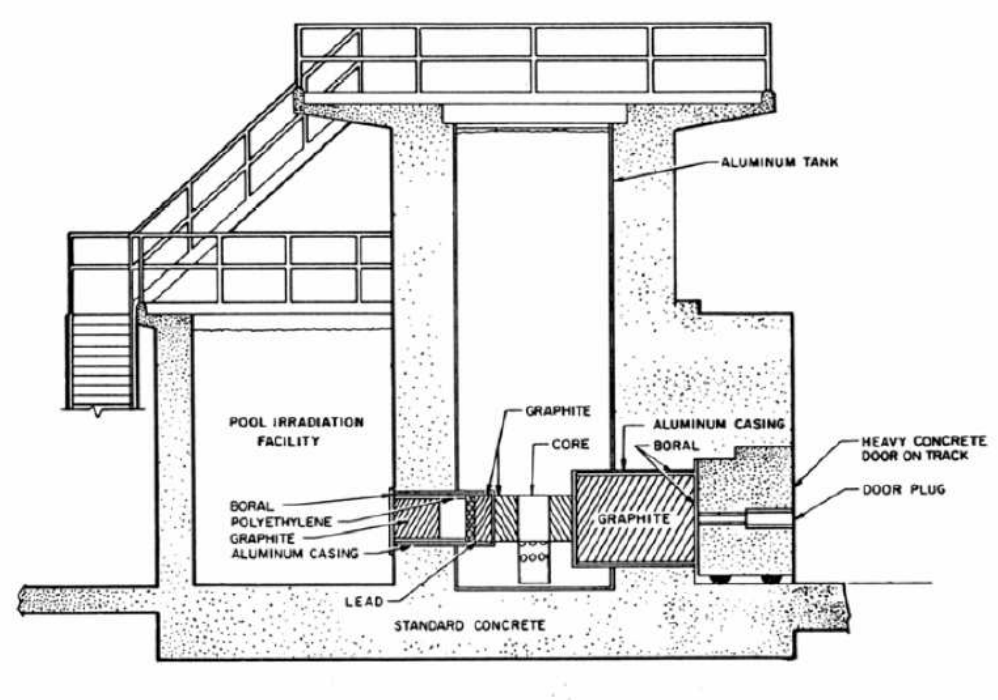

Figure 1. Side View of a TRIGA® Mark II reactor [6].

1.2.2 TRIGA® Fuel Design

The fuel elements in the OSTR are composed of low enriched uranium in a zirconium hydride matrix. The fuel also includes a burnable poison, erbium. The erbium has a double resonance at approximately 0.5 eV. As the fuel temperature increases, the resonance cross section appears to spread out and cover a wider range of energy [7]. As the temperature and resonance increase, thermal flux is depressed and the net reactivity decreases. This process is called Doppler broadening and is useful for adding stability to core reactivity.

Reactivity, an indicator of how many neutrons are available for fission within a reactor core, is defined as:

$$\rho = [k(t) - 1]/k(t) \qquad \textbf{Equation 1.}$$

where k is the time dependent multiplication factor [7]. If reactivity is less than zero, the core is subcritical and there are fewer neutrons in the following generation than the

previous. If reactivity is zero, there is one neutron produced from fission for every neutron in the previous generation and the reactor is critical. If reactivity is greater than zero, each neutron produces more than one neutron by fission and the reactor is supercritical. The amount of change in reactivity per change in degree of fuel temperature is the reactivity temperature coefficient:

$$\alpha = \frac{(\delta p/\delta T)}{p} \qquad \textbf{Equation 2.}$$

where p is the reactivity and T is the temperature. Reactors are required by the general design criterion of the Nuclear Regulatory Commission (NRC) to utilize a negative temperature coefficient within the power operating range [8].

The effect of the negative coefficient is that as the fuel heats up, the number of neutrons produced from each generation is reduced. The inherently safe design attained with a negative temperature coefficient is achieved by use of hydrogen moderator and erbium poison integrated within the fuel elements of TRIGA® reactors. In TRIGA ® reactors the negative temperature coefficient of the fuel will prevent further temperature increasing and ultimate meltdown. Although a LOCA will not result in fuel melting, the core would be uncovered creating a significant source term.

2. Literature Review

An analysis of the dose rate produced above the core as a result of a LOCA was performed in the OSTR SAR [9]. Two scenarios for LOCA were considered: 1) water pumped from the reactor tank and 2) reactor tank failure. The final determination was that the pump configuration for the OSTR could not result in complete loss of water from the tank. The water pump return pipe is above the top of the reactor core and will not drain water below the level of the reactor core. Thus, a reactor tank failure would be the main consideration for a LOCA.

Reactor tank failure could be caused by corrosion or mechanical failure of a joint on the reactor or an attached piping system. However, in the case of corrosion, the

leaks would be noticeable, and would undergo timely repair or an addition of water to the system to compensate for primary water loss. Mechanical failure could lead to extreme and irreversible loss of primary coolant from the reactor core. This could be caused by a sizeable object falling into the tank and irreparably damaging the tank wall, or the remote possibility of structural damage caused by and earthquake.

Once the core is uncovered there are two items that must be analyzed. The first is that the core will remain subcritical. Second is that dose rates in and around the facility do not exceed 10 CFR 20 regulations. The focus of this work is to estimate the source term and the resulting dose rates at points external to the reactor building in the event of an uncovered core.

The OSTR SAR utilized the activity equation from LaMarsh [10], equation 7, to determine the activity present in the core as a function of time after shutdown. The limitations of this equation are that it only applies to one fuel pin, and it only takes into account one operating cycle. If the reactor has been cycled on and off, long lived fission product buildup may skew the source activity. In the analysis the source was modeled as a cylinder, and the total activity was divided by the volume of the cylinder to determine the source flux. The fission product activity and source strength as calculated in the SAR are shown in Table 1.

Table 1. Fission Product Activity and Source Flux After Shutdown from the OSTR SAR.

Time After Shutdown	Fission Product Activity (Ci)	Flux/Core Height ($\gamma/cm^3 sec$)
10 seconds	8.15E+06	5.11E+12
1 hour	1.24E+06	7.78E+11
1 day	9.70E+05	6.08E+11
1 week	5.20E+05	3.26E+11
1 month	2.86E+05	1.79E+11

Once the source strength was determined, the dose rate at the reactor top was calculated using Equation 3:

$$\Phi = [S_v R^2/4\mu_c a^2][1-\exp(-\mu_c h)\ ] \qquad \textbf{Equation 3.}$$

where Φ is $\gamma\ cm^{-2}\ sec^{-1}$, S_v is the source flux per core height in $\gamma\ cm^{-3}\ sec^{-1}$, R is the core radius in cm, μ_c is the core attenuation coefficient ($1/cm^{-1}$), and h is the core height. Once the photon flux was calculated in $\gamma\ cm^{-2}\ sec^{-1}$, a dose conversion factor of $4.6x10^{-12}$ Sv $cm^2\ \gamma^{-1}$ was used to convert the flux to an effective dose equivalent rate. Table 2 shows the effective dose rates calculated in the OSTR SAR at the top of the cement bioshield. This methodology has also been used at other research reactor facilities [11].

Table 2. Effective Dose Rates at Reactor Top after Shutdown from the OSTR SAR.

Time After Shutdown	Effective Dose Equivalent Rate (rem/hr)
10 seconds	1.00E+04
1 hour	1.52E+03
1 day	1.19E+03
1 week	6.39E+02
1 month	3.51E+02

The following analysis will compare effective dose equivalent rates determined with MCNP5 analysis to the effective dose equivalent rates from the SAR.

An article by Patton H McGinley [12] examines dose rates calculated using equations from the National Council on Radiation Protection and Measurements (NCRP) Report # 51 [13]. The article compares photon and neutron measured dose rates at an 18 MeV medical accelerator with those calculated using equations from the NCRP Report #51. According to McGinley, the equations overestimate the photon dose rates up to approximately 10 meters. At distances greater than 10 meters, the calculated photon dose rates are underestimated. According to the data presented in the McGinley article, a correction factor would need to be determined for the facility before relying strictly on NCRP equations to determine dose rates external to the OSTR.

3. Background Theory

3.1 Fission Theory

Fission events produce fission fragments, neutrons, gamma rays and neutrinos. The fission fragments are charged particles since the fission process removes some of the electrons from the outer shells. The charged particles interact quickly within their surroundings, ionizing the atoms of the medium and losing energy. The neutrons, gamma rays and neutrinos are neutral in charge but behave differently. Neutral particles will travel in a straight trajectory until they collide with another particle. At this point they either are scattered or absorbed [7].

Neutrons are born with a distribution of energies, with an average energy of approximately 2 MeV, and may be characterized by their kinetic energy value. Neutron energies can be classified into three different neutron energies: fast, epithermal and thermal. Other energy ranges are defined, but fit within these three categories. Fast neutrons have an energy range from 0.01 to 10 MeV and their distribution, $\chi(E)$, is represented by Equation 5 [7]:

$$\chi(E)=0.453\exp(-1.036E)\sinh((2.29E)^{1/2}) \qquad \textbf{Equation 5.}$$

where E is the energy in eV. The epithermal neutron energy range is approximately 1 to 10 keV, whereas thermal neutrons have energies less than 1 eV. Thermal neutron energy distribution is ideally characterized by the Maxwell-Boltzmann equation:

$$M(E)=\frac{2*\pi*E^{1/2}}{(\pi kT)^{3/2}}\exp(-E/kT) \qquad \textbf{Equation 6.}$$

where E is the energy in eV, T is the temperature in K, and k is the Boltzmann Constant of $8.617\text{x}10^{-5}$ eV/K [7]. The energy ranges presented here are not definite values and may vary depending upon the definition.

In the case of the TRIGA reactor at OSU, the neutrons produced are moderated by the uranium hydride fuel and the primary coolant. Thermalized neutrons that diffuse in the core or re-enter the core from the primary coolant may go on to produce fission within the fuel.

During fissioning, the target nucleus will split into two different nuclei. When a thermal neutron causes fission, there is a well defined difference between the masses of the two newly created nuclei. If the neutron energy is greater than a few eV, the nuclei may split where the mass is distributed more equally. Figure 2 below depicts the dip in the fission yield curve for thermal energies, and the flattening of the curve for higher energy neutrons.

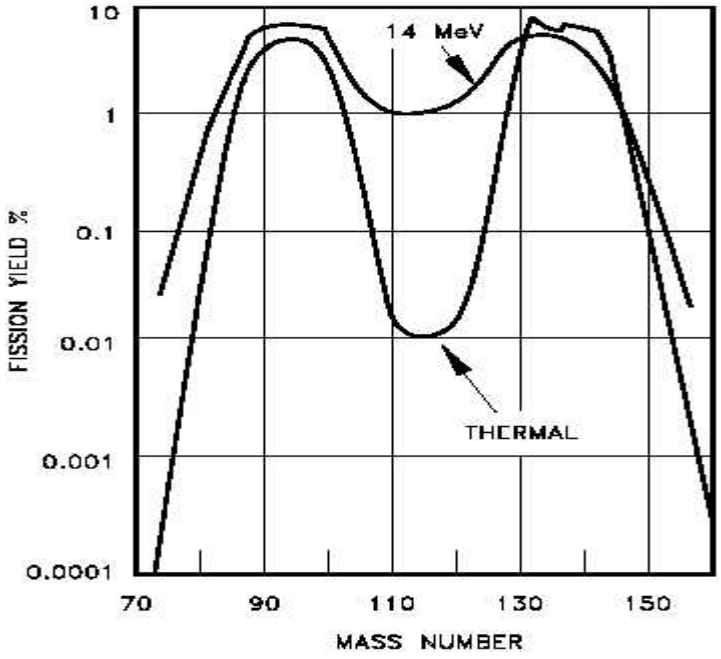

Figure 2. Uranium 235 Fission yield vs. mass number [14].

Lower atomic number isotopes have a neutron to proton ratio of 1:1. As atomic number increases, the isotopes reach stability with a higher number of neutrons than protons. Shown in Figure 3, the fission fragments created from fission typically do not have a stable ratio of neutrons to protons; therefore they will decay to reach the line of stability.

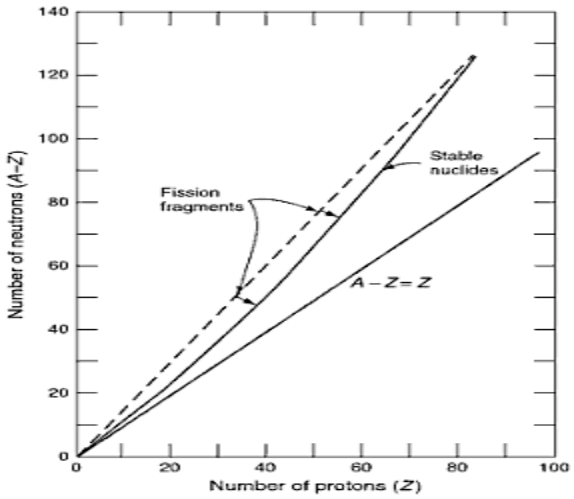

Figure 3. Fission fragment instability diagram [9].

Each daughter product of the fission fragment decay has a different decay half life. Thus, the time required to reach stability is different for each isotope created through fission [7].

3.2 Fission Product Decay Activity

The activity in curies produced by the decay products may be calculated by the following:

$$A(t)= 1.4x10^{6} P[t^{-0.2} – (t+T)^{-0.2}] \qquad \textbf{Equation 7.}$$

where P is the reactor thermal power (MW), t is the time after shutdown in days, and T is the operating time prior to shutdown [10].

The OSTR operates approximately 7 hours per weekday at 1 MW power. Plotting Equation 7 versus time with a 7 hour reactor operating time gives the decay shown in Figure 4.

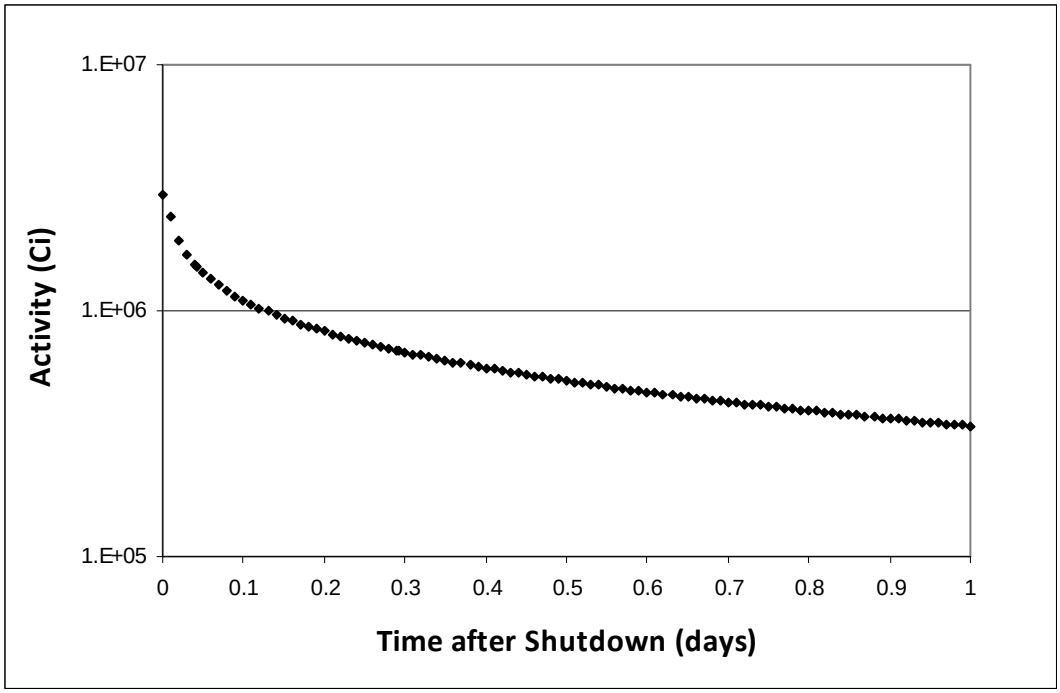

Figure 4. Fission product activity as a function of time after OSTR shutdown.

Using equation 7 with a 7 hour operating time the activity of the OSTR core is calculated to be 1.79 MCi at end of bombardment (EOB). During shut down the fission products decay, but longer lived isotopes do not completely dissipate. The next operating cycle adds to the amount of longer half life isotopes produced. The decay activity resulting from these longer lived isotopes causes a shift in the plot to a higher activity value than one would see if a reactor was shut down after constant operation.

3.3 Electromagnetic Radiation

Photons are the quantum of energy which comprises electromagnetic radiation (EMR) [15]. Photons have no mass, no charge, and travel at the speed of light. EMR classification depends upon the wavelength and frequency of the wave generated. Figure 5 shows the range of EMR and classification as a function of wavelength.

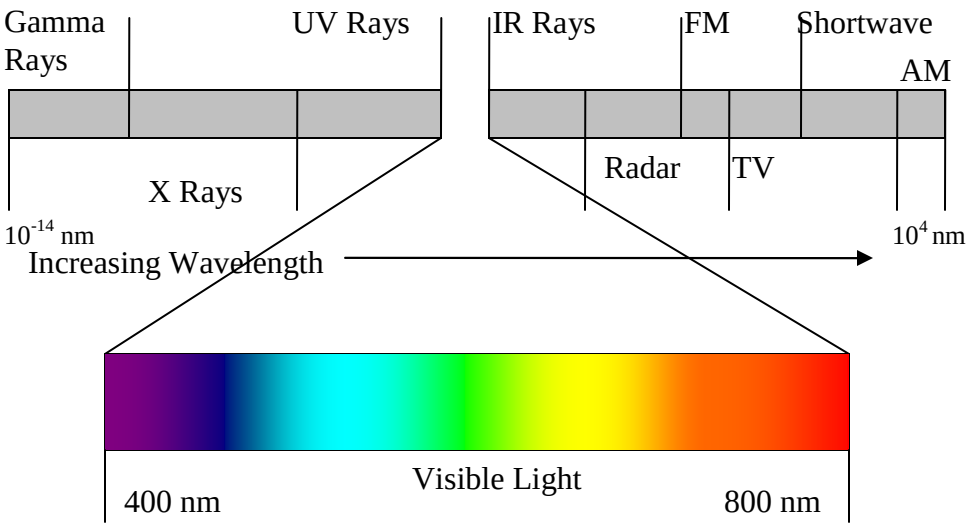

Figure 5. Electromagnetic energy spectrum.

Photon energies are inversely proportional to their wavelength. The relationship between energy and wavelength is given by:

$$E=hc/\lambda \qquad \textbf{Equation 8.}$$

where h is Planck's constant, c is the speed of light, and λ is the wavelength.

Photons interact with the medium by absorption and scatter. Once photons have traveled through a medium, scattering may result in photons of a different energy or a different angle than the original photon beam [15]. Photons may travel a long distance in a medium before interacting, so they are the primary concern for estimating dose from uncovering of the OSTR. Photon interaction mechanisms are discussed further in the next section.

3.4 Shielding and Photon Interactions

The water surrounding the OSTR reactor core provides shielding for the emitted radiation, cooling for the reactor core and neutron moderation. Radiation traveling through a medium undergoes either geometric or material attenuation. Geometric

attenuation occurs when a given number of particles disperse into a larger volume of medium. Material attenuation occurs when the photons are absorbed from the incident photon beam, or scatter in a direction away from that of the incident photon beam [15].

To accurately describe the total attenuation through a material, both material and geometric attenuation must be taken into account. Once the photons have been scattered, they will enter a detector at an angle different from the initial beam angle or be scattered away from a detector. Radiation flux decreases in a material exponentially according to Equation 9:

$$I(x)=I(0)Be^{-\mu x} \qquad \textbf{Equation 9.}$$

where I is the flux, B is the buildup factor, μ is the linear attenuation coefficient and x is the distance the photon travels through the medium. The buildup factor is a correction factor based on the thickness and energy of the photons interacting with in a material. The correction factor takes into account photons that are scattered back toward the detector but are not taken into account by use of the linear attenuation coefficient alone.

3.4.1 Photoelectric Effect

Photoelectric effect occurs when a photon transfers sufficient energy to an inner shell electron, thus ejecting the electron from the atom [15]. The kinetic energy of the electron is equal to the energy of the incident photon minus the electron binding energy:

$$T = E_\gamma - B_e \qquad \textbf{Equation 10.}$$

where E_γ is the energy of the incident photon and B_e is the binding energy [16]. The probability of the photoelectric effect increases with increasing atomic number, Z, and with lower energy photons. Typically the photons that undergo this type of interaction are less than 0.5 MeV.

3.4.2 Pair Production

Pair production occurs when a photon traversing a high electromagnetic field is converted into an electron positron pair. The energy of the incident photon must exceed 1.022 MeV to provide the rest mass energy of the electron and positron. The kinetic energy divided between the remaining electron and positron pair is:

$$T_- + T_+ = E_\gamma - 2mc^2 \qquad \textbf{Equation 11.}$$

where $2mc^2$ is 1.022 MeV [16]. The positron electron pair will create ionizations in the surrounding material along their path. The greater the initial energy, the more energy is transferred to the surrounding medium. As the positron slows down, it will become attracted to an electron and will annihilate, producing two 511 keV gamma rays. The resulting gamma rays will continue within the medium, in exactly opposite directions [15].

3.4.3 Compton Scattering

Photons traveling through a medium with loosely bound outer electrons may undergo Compton scattering. The probability of interaction decreases as the photon energy decreases, and increases as the atomic number increases. In Compton scattering, the incoming photon collides with an outer shell electron. The collision transfers part of the photon energy to the electron, and both particles subsequently scatter. The kinetic energy of the electron after collision is dependent upon the initial photon energy and the scatter angle, and is calculated by Equation 12:

$$KE_e = \frac{(h\nu)}{m_o c^2} \cdot \frac{h\nu(1-\cos\theta)}{[1+h\nu/\, m_o c^2\,(1-\cos\theta)]} \qquad \textbf{Equation 12.}$$

The maximum kinetic energy occurs when the scattering angle is 180° [15].

3.4.4 Coherent Scattering

Coherent scattering occurs when the incident photon wavelength is much greater than the radius of the atom or molecules they strike. The result is that the emitted photon will continue to travel at the same energy as before the collision. Coherent scattering differs from the previously mentioned types of scattering in that it: 1) does not result in a different particle emitted from the atom and 2) results in retention of all energy by the incident photon.

3.5 Ionization Chambers

An ion chamber is a type of detector that depends upon interactions within a gas medium to create ion pairs. Ion pairs are created as the radiation interacts within the gas by depositing energy and ionizing the atoms. The minimum amount of energy required to remove an electron from its shell ranges from 10 to 25 eV depending on the type of gas; however, not all energy deposited by the radiation results in the removal of an electron from its shell.

There are several factors that can reduce the number of ion pairs formed within the gas, including recombination and electron attachment. Recombination occurs when positive and negative ions join together to create neutral atoms. Electron attachment effectively reduces the number of free electrons in the ion chamber. As the electrons diffuse through the gas, a high electron affinity gas may attract electrons to a neutral atom. The result is an increase in negative ions within the gas.

To overcome the overall reduction in ion pairs, an electric field is applied to the ion chamber. The field induces separation of the negatively and positively charged particles. The oppositely charged particles migrate to electrodes, creating a current in the detector. The magnitude of the current produced is proportional to the number of ion pairs that are formed from ionization of the gas.

To account for the average energy lost to events that do not result in ion pairs, W-values were created. The W-value is a correction factor that takes into account the

type of radiation and the chamber gas. Knowing the W-value for the specified ion chamber gas and type of radiation, the energy of incident radiation can determined from the number of ion pairs formed [17].

3.6 Dose and Dose Equivalent

Absorbed dose is the amount of energy from ionizing radiation deposited in a given medium [15]. The units of absorbed dose are rad, or gray in SI units. The absorbed dose is converted to dose equivalent in units of rem, or sieverts in SI units, by a quality factor. The quality factor takes into account the effectiveness of the radiation as compared to a standard low LET radiation.

For this research, the exposure values measured at distances above the reactor core are a starting point to calculate the dose rate. The exposure can either be measured with a detector or estimated using analytical methods. Once the exposure is determined, it is converted to rad by Equation 13:

$$1\ R = 0.877\ \text{rad (in air)} = D\ \text{(absorbed dose)} \qquad \textbf{Equation 13.}$$

where R is the measured or calculated exposure. A rad is the equivalent to 100 ergs of energy absorbed in 1 gram of absorbing medium [15].

The amount of biological damage incurred from radiation depends upon the type of incident radiation. Radiation that has a high linear energy transfer (LET) will do more damage than radiation with a low LET. A high LET radiation will deposit more energy over a given linear amount of tissue than a low LET radiation. To account for the differences in energy transfer rates, the absorbed dose is multiplied by a weighting factor to determine the dose equivalent.

$$H = D * Q \qquad \textbf{Equation 14.}$$

where H is the dose equivalent in rem, D is the absorbed dose in rad, and Q is the weighting factor.

To determine the dose rate over a specified amount of time, the activity from equation 7 is integrated to give

$$\int A(t)dt = P\left[\, 1.75E{+}6 \times t^{-.8} - 1.75E{+}6 \times (t+T)^{0.8} \,\right] \qquad \textbf{Equation 15.}$$

where t is the time of interest, and T is the reactor operating time prior to shutdown. The integrated activity is then taken and substituted into equation 18 to give an exposure rate in R/hr. The dose rate is then calculated using equation 13.

3.7 Skyshine

Skyshine occurs when radiation traveling in an upward direction is scattered off of atoms in the atmosphere and travel back toward the earth [18]. In the case of a TRIGA reactor, the core is shielded with sixteen feet of water which attenuates the majority of the radiation produced. However, a LOCA would change the attenuating medium from water to air, significantly reducing the magnitude of the attenuation coefficient. Thus photons traversing a given distance in air would undergo less attenuation than photons traversing the same distance in water.

3.8 MCNP5

MCNP5, Monte Carlo N-Particle, was used to simulate the photon flux from the core and energy deposition in volumes of interest. Monte Carlo methods were originally developed by scientists at Los Alamos National Laboratory during the 1940s [19]. Monte Carlo (MC) methods are mathematically rigorous, and were first made practical for predicting particle transport with the invention of the computer. Computers allowed the multitude of calculations required for MC simulations to be performed in a reasonable time frame. The first version of MCNP was written in 1963, called MCS[18]. Through the years the code was increased in complexity with added particle types and broadening energy value ranges. In the 1970s, eigenvalue algorithms were added to determine k_{eff}.

MCNP simulates particle histories individually from birth to death, terminating each particle upon absorption or exiting the geometry. MCNP allows the user to define the particle transported in a specified geometry. The particle will start in an identified source point, area or volume. The user assigns the particle a given weight and energy. The direction of travel is then randomly selected. To determine the distance a particle travels, the probability of interaction along a given length is calculated by:

$$p(\ell) = \int e^{-\Sigma t \ell} \Sigma_t d\ell \qquad \textbf{Equation 16.}$$

where $p(\ell)$ is the probability of interaction from ℓ to $\ell + d\ell$, and Σ_t is the total cross section. The probability is equal to a random number from zero to 1, ξ. The distance to the next interaction is then given by:

$$\ell = -(1/\Sigma t)*\ln(\xi) \qquad \textbf{Equation 17.}$$

Once the particle interacts, the type of collision is identified. The type of interaction is also determined by random probability based on the absorption, scattering and total cross sections. After the current particle terminates, the next particle is started and a new history is tracked.

The geometry is composed of surfaces and cells, in which surfaces are combined to create cells. The cells are defined by space that has a positive or negative directional relationship to each surface. Once the geometry has been created, the outside universe must be defined as a void. A void is a cell or cells with no material or cross section defined. Once the particle enters the void, the particle is terminated.

4. Materials and Methods

4.1 Exposure Measurements

In order to estimate the activity of the core, exposure measurements were taken using a Technical Associates model CP-MU ion chamber at six different heights above the core [20]. The ion chamber position relative to the core is shown in Figure 6.

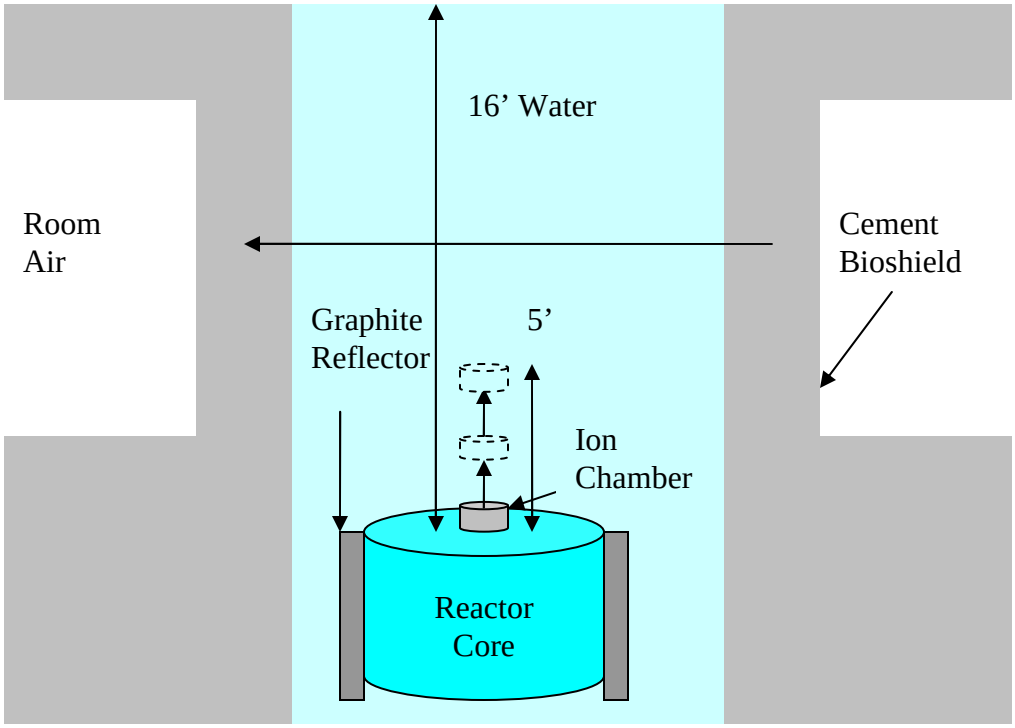

Figure 6. Ion chamber placement above reactor core.

During the measurements, the primary water surrounded the core as removing the water for testing is unfeasible. The results of the exposure measurements at various heights are given in Table 3 [20].

Table 3. Measured exposure rates at points above the OSTR.

Description	Measured Exposure [R/hr]
Top of core	1000 ± 100
1 ft above core	360 ± 100
2 ft above core	72 ± 10
3 ft above core	10 ± 1
4 ft above core	2 ± 0.1
5 ft above core	0.4 ± 0.01

As expected, the measurements show an exponential decrease with distance. To determine the error of each measurement, the minimum ascertainable readout from the ion chamber meter was determined. The range for minimum and maximum values

was then determined by adding and subtracting the minimum measurement reading from the measured value. The measured exposure values were taken in 1999 during a routine survey of the reactor. There was only one set of exposure values taken at the time. Taking measurements to repeat for statistical accuracy would induce error by the measurement technique since the same employee is no longer available to repeat the measurements exactly.

4.2 TRIGA Reactor Modeling

MCNP5 was used to create a simplified model of the OSTR. The model includes the basic geometries of the core, primary coolant, ion chambers, bioshield, surrounding room air, facility building and air above and lateral to the reactor building. A complete MCNP5 input deck is provided in Appendix A.

The core was modeled as a cylindrical volume surrounded by water, cement, and room air. The fine details of the core, such as individual fuel elements and control rods, were not included. The assumptions made for the geometry and source were reasonable since the purpose of the source modeling was to determine a photon distribution and source activity. The ion chamber was modeled as a small cylindrical volume placed at specific heights above the core.

The bioshield and structure support were modeled as three different layers. The bottom layer was modeled as a rectangular base, with a cylinder of core material and water directly in the center. The middle layer is a cylinder of water surrounded by a cylinder of cement. The third layer is similar to the bottom layer with a rectangular shape concrete slab and a cylindrical water center. Figures 7 and 8 are side and top views of the OSTR model.

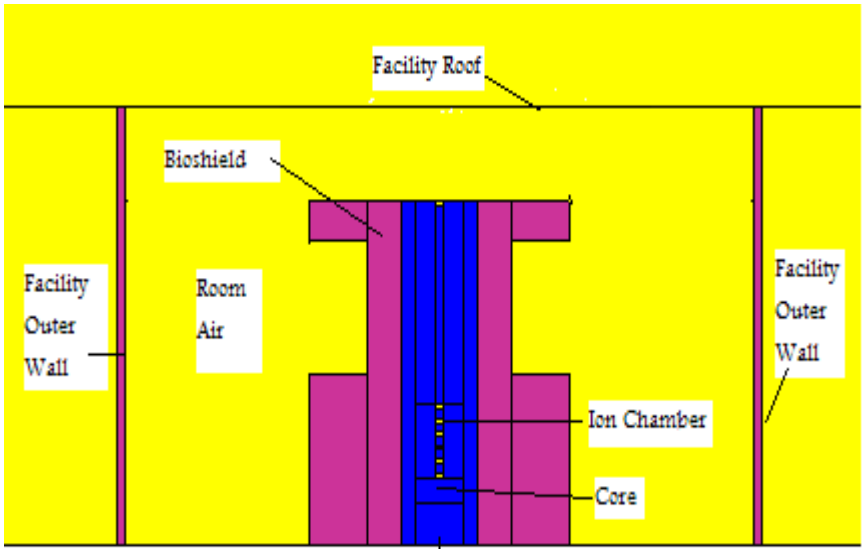

Figure 7. Side Vertical view of the OSTR model.

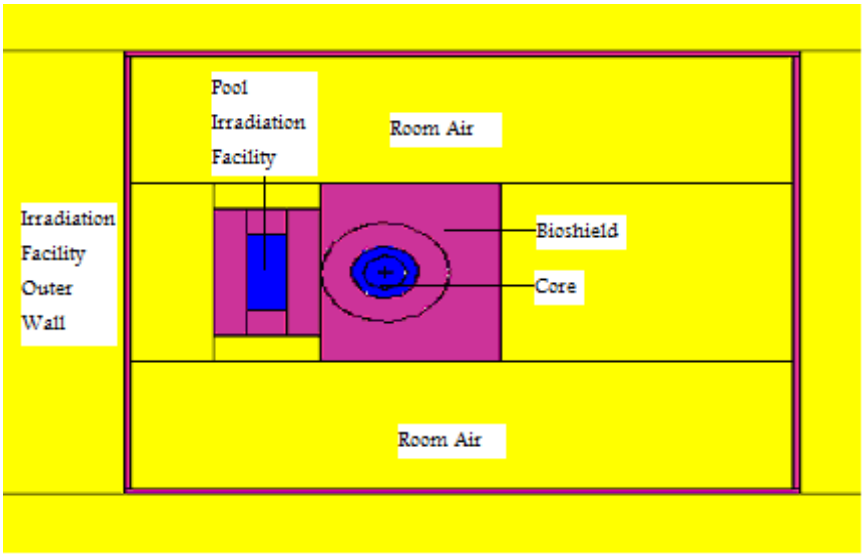

Figure 8. Top view of the OSTR model.

The true octagon shapes of the base and top were modeled as rectangles for ease of modeling. The material thickness of the base, beyond a few inches, is not considered significant since the photons would be attenuated significantly prior to reaching the narrowest width of cement. Also, attenuation from the aluminum housing of the ion chamber was neglected.

4.2.1 Material Specification

The four materials specified for the model of the OSTR and surroundings are given in Table 4.

Table 4. Material compositions for MCNP5 model.

Material Number	Material	Material Component	Atom Percent
1	Cement	Calcium	31.3%
		Oxygen	55.7%
		Silicon	10.1%
		Aluminum	2.2%
		Iron	.7%
2	Water	Hydrogen	66.7%
		Oxygen	33.3%
3	Air	Nitrogen	75%
		Oxygen	25%
4	Stainless Steel (304)	Iron	70%
		Carbon	8%
		Chromium	18%
		Manganese	1%
		Silicon	1%
		Phosphorus	1%
		Sulfur	1%

The air was modeled with nitrogen and oxygen because together they account for greater than 99% of the mass percent of air.

4.2.2 Tally Specification

The tally type used in MCNP5 was a *F8 tally. The F8 tally sums the number of interactions of a certain energy deposited in a cell. The "*" modifier in front of the F8 changes the tally by tracking and summing the energy deposited per initiated particle in the volume of interest [19]. The *F8 tally was chosen because absorbed dose can easily be calculated from the results which are given in units of MeV per initial photon.

Only photon energy deposition is considered important in this analysis. Once the LOCA occurs, the large negative temperature coefficient of the reactor fuel effectively shuts off the fission reactions within the core. Charged particle deposition is ignored since they interact with the surrounding atoms and come to rest after relatively short distances compared to the photons.

4.2.3 Source Specification

Of particular importance is the energy distribution of the photons. The source was modeled as a photon emitting cylinder. Multiple simulations were run with varying initial photon energies for each simulation. The first six simulations were run with monoenergetic photons. The seventh simulation used a Maxwellian distribution and simulations 8 through 13 were run with a distribution of energies from 1 to 10 MeV. The distributions were based on percentages determined from the monoenergetic photon simulations. The distributions are described further in section 5.2. Table 5 lists the energy values used for each simulation.

Table 5. Initial photon energy values for MCNP5 simulations.

Simulation		Energy Values
1	Monoenergetic	1 MeV
2	Monoenergetic	2 MeV
3	Monoenergetic	3 MeV
4	Monoenergetic	5 MeV
5	Monoenergetic	7.5 MeV
6	Monoenergetic	10 MeV
7	Maxwellian	Maxwellian Distribution
8	Distribution 1	Distribution 1 to 10 MeV
9	Distribution 2	Distribution 1 to 10 MeV
10	Distribution 3	Distribution 1 to 10 MeV
11	Distribution 4	Distribution 1 to 10 MeV
12	Distribution 5	Distribution 1 to 10 MeV
13	Distribution 6	Distribution 1 to 10 MeV

5. Results

5.1 Exposure Rates – Monoenergetic Photons

MCNP5 simulations 1 through 6 were run using monoenergetic photon energies, with and without the primary water present. The source activity was calculated with water, based on the energy deposited in the cell positioned directly above the reactor core. The simulation including the primary water was used to determine the source activity because the exposure measurements were taken while the core was surrounded by primary coolant. The activity was then calculated by:

$$A = \frac{E}{[PE*J*100\ rad/Gy]/[.877rad/R*M]} \qquad \textbf{Equation 18.}$$

where A is the activity in photons per hour, E is the exposure in R per hour, PE is the *F8 tally results in MeV per initial photon, J is a MeV to Joules conversion factor of $1.6x10^{-13}$, M is the mass of each cell in kg.

The tally for the cell directly on the core top had the lowest error due to the largest number of particles deposited in the cell. After the core activity was determined using the energy deposited in the cell directly on top of the core, equation 18 was rearranged to solve for E of the remaining cells simulating the ion chamber. Tables 6 and 7 provide the source activity and calculated exposure rates in comparison to the measured exposure rates for simulations 1 through 6, with and without water. Figures 9 and 10 are graphs of exposure rates calculated from the monoenergetic photon energy simulations versus the measured exposure values. The measured values are the same in both graphs; however, the calculated values differ by simulation with or without primary water.

Table 6. Source activity and calculated exposure rates for monoenergetic photon energies in water.

		1 MeV		2 MeV		3 MeV	
Position	**R/hr (Measured)**	**Source Activity (γ/hr)**	**R/hr (Calculated)**	**Source Activity (γ/hr)**	**R/hr (Calculated)**	**Source Activity (γ/hr)**	**R/hr (Calculated)**
Top of core	1000 ± 100	5.47E+17	1000 ± 0.30	3.49E+17	1000 ± 0.30	2.61E+17	1000 ± 0.30
1 ft above core	360 ± 100		37.9 ± 0.04		48.86 ± 0.054		55.6 ± 0.067
2 ft above core	72 ± 10		3.4 ± 0.01		6.67 ± 0.019		9.19 ± 0.26
3 ft above core	10 ± 1		0.34 ± 0.003		1.096 ± 0.0076		1.86 ± 0.011
4 ft above core	2 ± .1		0.053 ± 0.004		0.26 ± 0.0036		0.536 ± 0.006
5 ft above core	0.4 ± 0.01		0.006 ± 0.0004		0.05 ± 0.0016		0.132 ± 0.003
Reactor Top			0 ± 0.00		0.0 ± 0.0		0.00 ± 0.00
		5 MeV		**7.5 MeV**		**10 MeV**	
Position	**R/hr (Measured)**	**Source Activity (γ/hr)**	**R/hr (Calculated)**	**Source Activity (γ/hr)**	**R/hr (Calculated)**	**Source Activity (γ/hr)**	**R/hr (Calculated)**
Top of core	1000 ± 100	1.82E+17	1000 ± 0.400	1.35E+17	1000 ± 0.4	1.08E+17	1000 ± 0.4
1 ft above core	360 ± 100		63.1 ± 0.082		67.7 ± 0.095		99.2 ± 0.14
2 ft above core	72 ± 10		12.4 ± 0.035		14.68 ± 0.04		15.9 ± 0.05
3 ft above core	10 ± 1		3.12 ± 0.017		4.16 ± 0.02		4.8 ± 0.024
4 ft above core	2 ± .1		1.08 ± 0.0096		1.6 ± 0.013		1.96 ± 0.15
5 ft above core	0.4 ± 0.01		0.337 ± 0.005		0.55 ± 0.007		0.72 ± 0.009
Reactor Top			0.00 ± 0.00		0.00 ± 0.00		0.00 ± 0.00

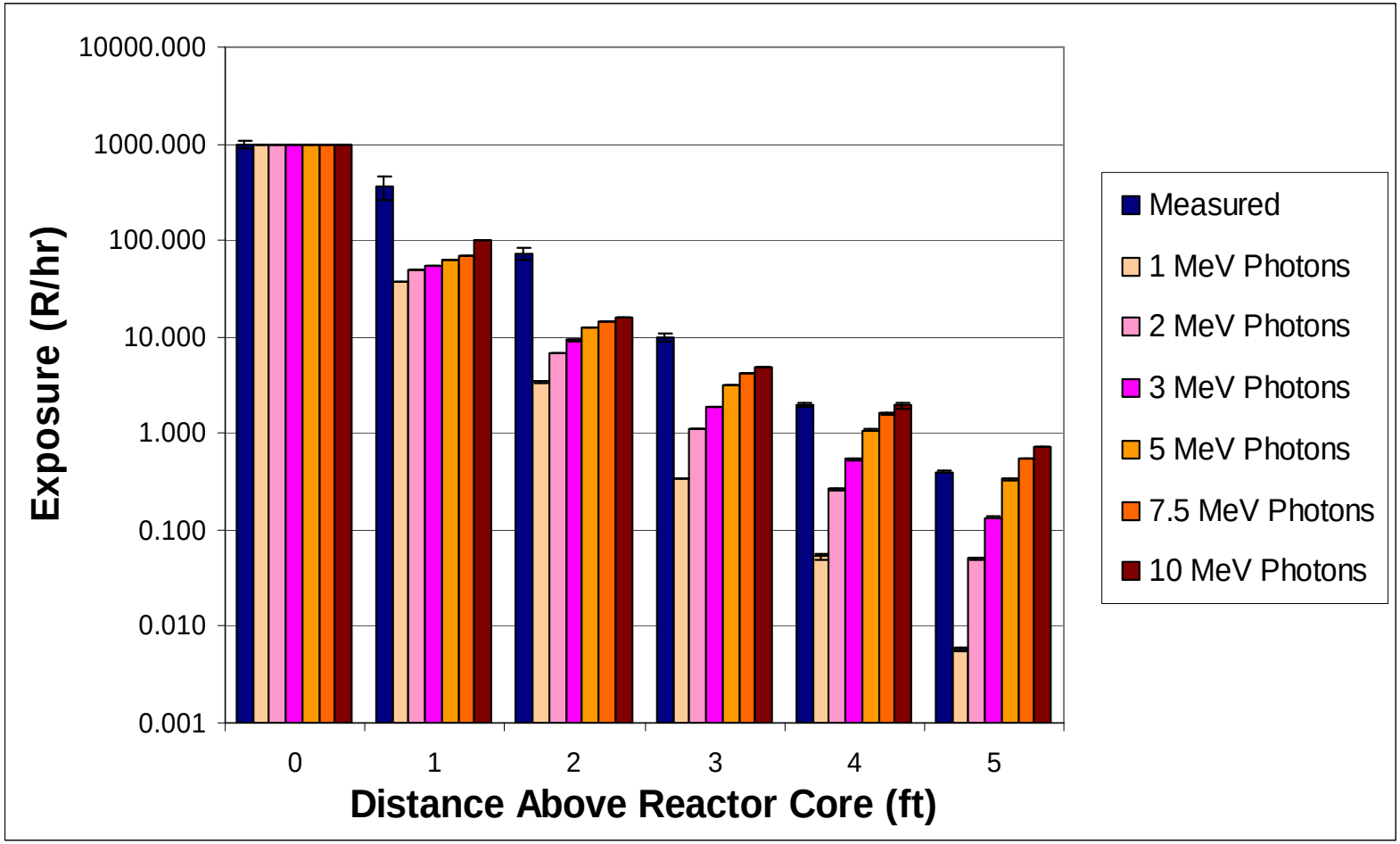

Figure 9. Exposure rates calculated from MCNP5 results in water.

Table 7. Source activity and calculated exposure rates for monoenergetic photon energies in air.

		1 MeV		2 MeV		3 MeV	
Position	**R/hr (Measured)**	**Source Activity (γ/hr)**	**R/hr (Calculated)**	**Source Activity (γ/hr)**	**R/hr (Calculated)**	**Source Activity (γ/hr)**	**R/hr (Calculated)**
Top of core	1000 ± 100		1000 ± 7.00		1000 ± 8.10		1000 ± 8.8
1 ft above core	360 ± 100		112 ± 2.30		109 ± 2.65		104 ± 2.79
2 ft above core	72 ± 10		43.6 ± 1.44		44.1 ± 1.7		42.5 ± 1.81
3 ft above core	10 ± 1	5.47E+17	22.6 ± 1.01	3.24E+17	21.5 ± 1.16	2.38E+17	20.1 ± 1.22
4 ft above core	2 ± .1		14.7 ± 0.81		14.2 ± 0.94		14.12 ± 1.02
5 ft above core	0.4 ± 0.01		10.2 ± 0.65		9.8 ± 0.77		9.54 ± 0.83
Reactor Top			0.84 ± 0.19		0.93 ± 0.23		0.60 ± 0.18
		5 MeV		**7.5 MeV**		**10 MeV**	
Position	**R/hr (Measured)**	**Source Activity (γ/hr)**	**R/hr (Calculated)**	**Source Activity (γ/hr)**	**R/hr (Calculated)**	**Source Activity (γ/hr)**	**R/hr (Calculated)**
Top of core	1000 ± 100		1000 ± 9.6		1000 ± 10.1		1000 ± 10.3
1 ft above core	360 ± 100		105 ± 3.11		107 ± 3.3		367 ± 11.5
2 ft above core	72 ± 10		42 ± 1.96		41 ± 2.04		41.4 ± 2.08
3 ft above core	10 ± 1	1.61E+17	19.5 ± 1.33	1.12E+17	19.3 ± 1.38	8.48E+16	19.2 ± 1.4
4 ft above core	2 ± .1		13.9 ± 1.12		13.9 ± 1.17		13.8 ± 1.19
5 ft above core	0.4 ± 0.01		10.1 ± 0.95		10.1 ± 1.01		9.9 ± 1.01
Reactor Top			0.58 ± 0.21		0.61 ± 0.22		0.56 ± 0.21

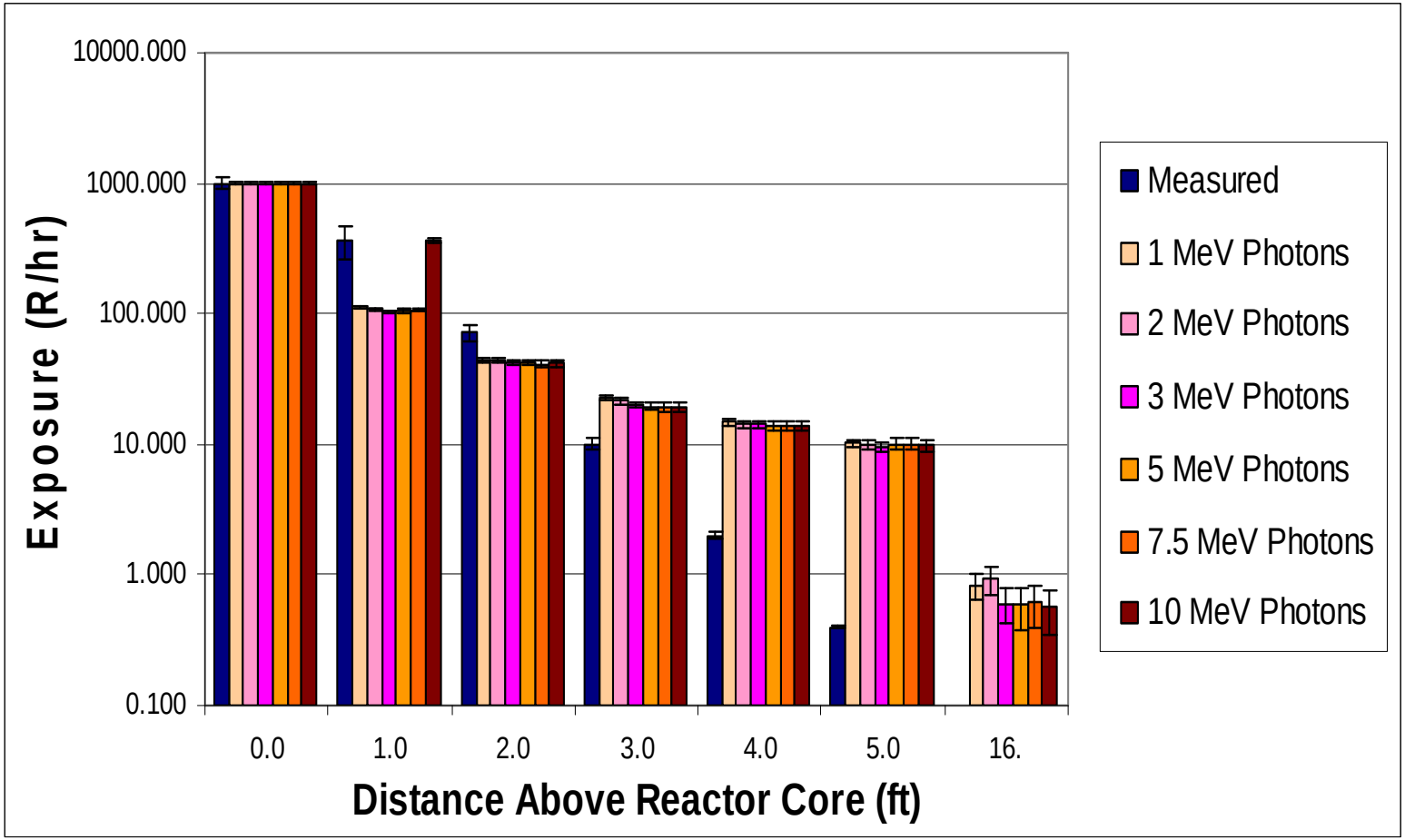

Figure 10. Exposure rates (R/h) at various heights above the TRIGA reactor core in air.

The exposure levels simulated in water did not exceed the measured values. However, the exposure levels in air exceeded measured values as the distance above the core increased. The larger energy deposition in air cells farther from the core occurred because the photons underwent fewer collisions in the air medium, thus retaining greater amounts of their initial energy at greater distances from the core.

The *F8 tally results that would be required to equal the measured exposure values were back calculated using Equation 18. The energies per photon that would equate to the measured exposure values are displayed in Table 8.

Table 8. *F8 tally equivalent to the measured exposure values.

	*F8 Tally Equivalent [MeV/photon]		
Position	**1 MeV**	**2 MeV**	**3 MeV**
Top of Core	3.9580E-05	6.6843E-05	9.0926E-05
1 ft above	1.4249E-05	2.4063E-05	3.2733E-05
2 ft above	2.8498E-06	4.8127E-06	6.5467E-06
3 ft above	3.9580E-07	6.6843E-07	9.0926E-07
4 ft above	7.9160E-08	1.3369E-07	1.8185E-07
5 ft above	1.5832E-08	2.6737E-08	3.6370E-08
Reactor Top	3.3158E-08	6.2386E-08	5.4795E-08
Position	**5 MeV**	**7.5 MeV**	**10 MeV**
Top of Core	1.3445E-04	1.9258E-04	2.5514E-04
1 ft above	4.8403E-05	6.9328E-05	9.1849E-05
2 ft above	9.6805E-06	1.3866E-05	1.8370E-05
3 ft above	1.3445E-06	1.9258E-06	2.5514E-06
4 ft above	2.6890E-07	3.8515E-07	5.1027E-07
5 ft above	5.3781E-08	7.7031E-08	1.0205E-07
Reactor Top	7.8605E-08	1.1826E-07	1.4299E-07

The *F8 tally results equivalent to the measured exposure rates were then plotted with the MCNP5 simulated *F8 tally results for each monoenergetic photon source. The plots are shown in Figures 11 through 16, below.

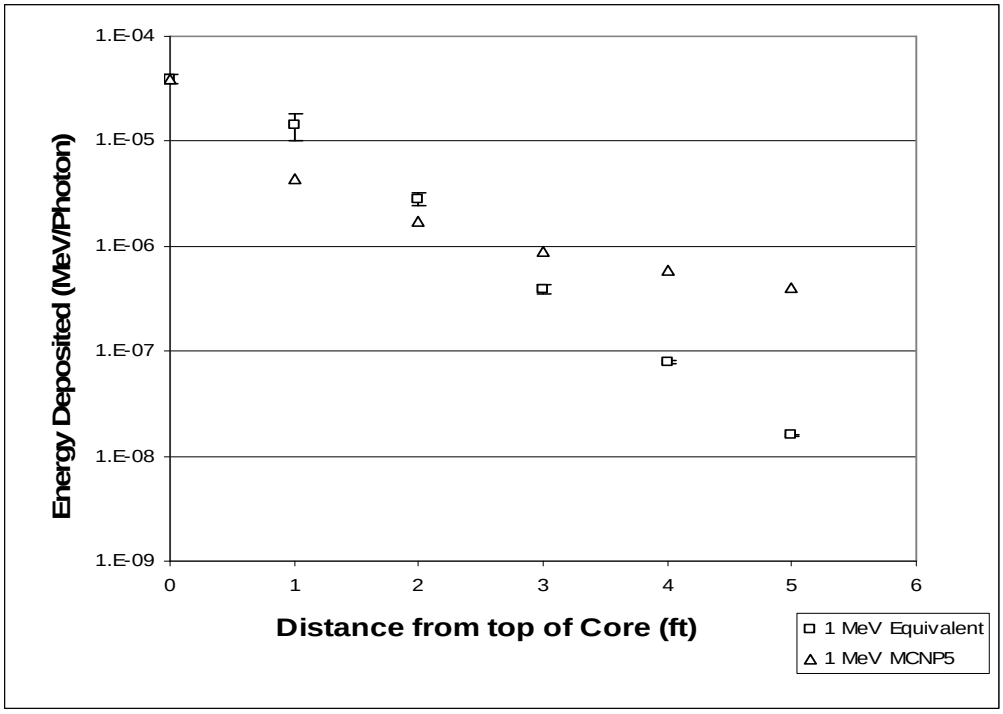

Figure 11. Energy deposited by 1 MeV photons in a simulated ion chamber as a function of distance from the core.

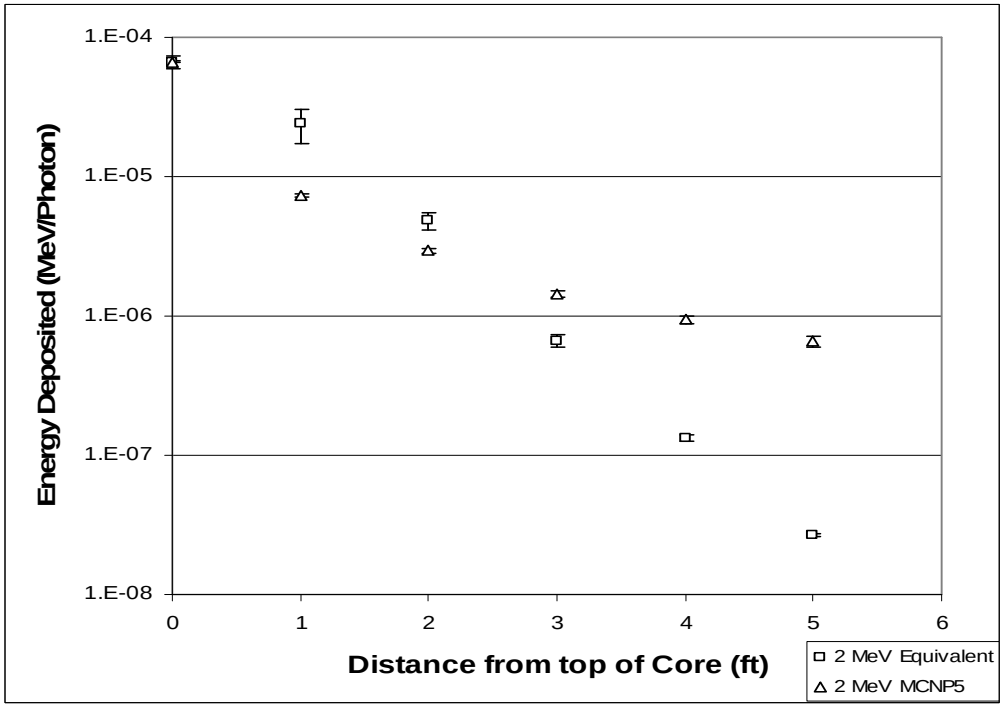

Figure 12. Energy deposited by 2 MeV photons in a simulated ion chamber as a function of distance from the core.

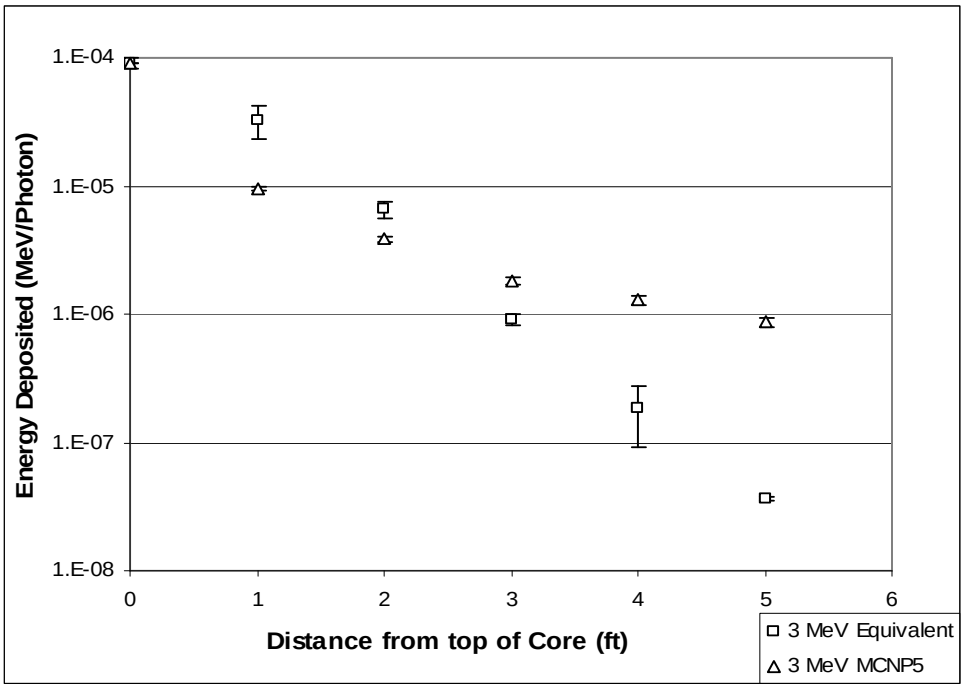

Figure 13. Energy deposited by 3 MeV photons in a simulated ion chamber as a function of distance from the core.

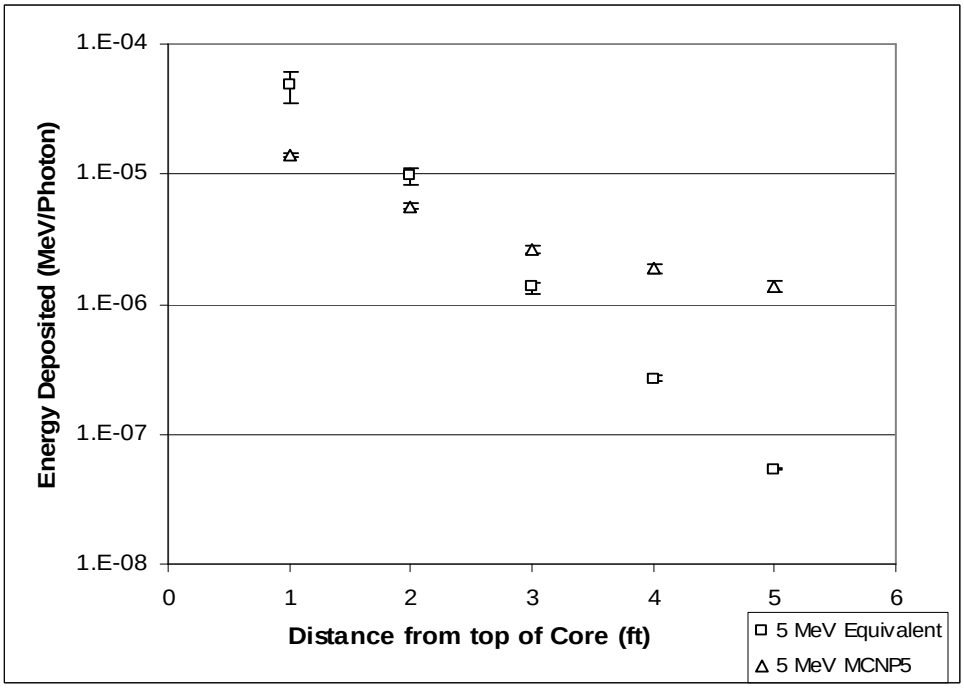

Figure 14. Energy deposited by 5 MeV photons in a simulated ion chamber as a function of distance from the core.

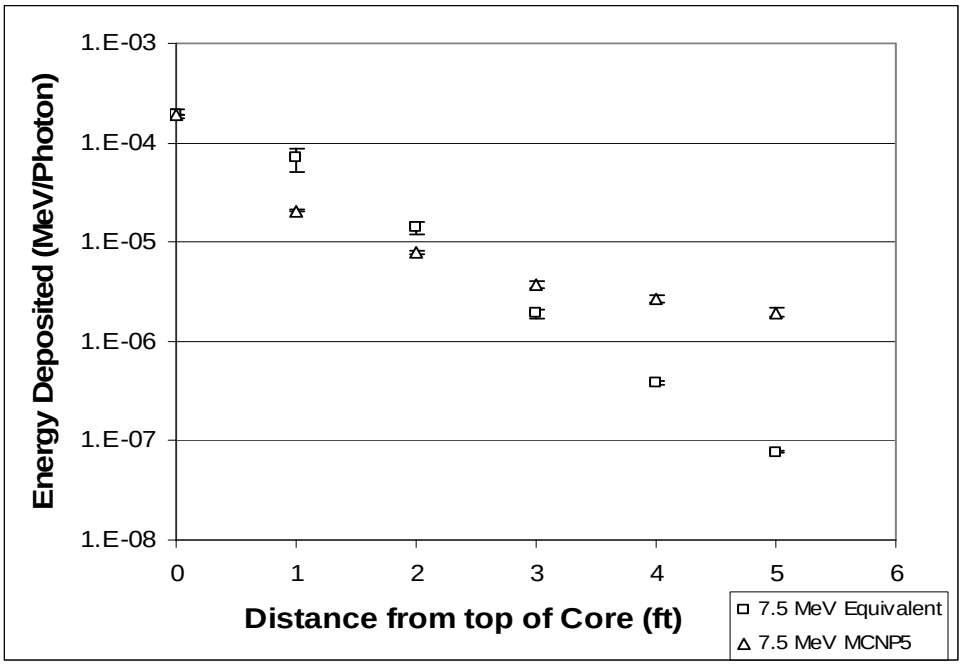

Figure 15. Energy deposited by 5 MeV photons in a simulated ion chamber as a function of distance from the core.

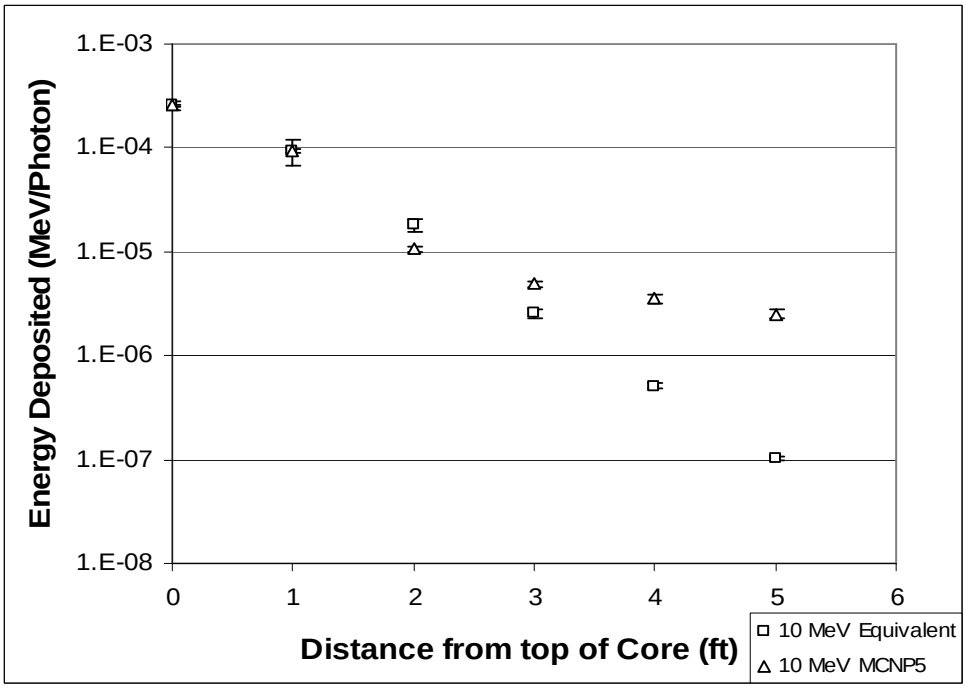

Figure 16. Energy deposited by 10 MeV photons in a simulated ion chamber as a function of distance from the core.

The height at which the plots intersect is approximately 2.7 ft above the core in each case. This height represents the average height required for the number of interactions simulated to be equivalent to the number of interactions equaling the measured exposure values. The number of interactions that occurred in each ion chamber cell was divided by the total number of initiated particles - 300,000,000 for each simulation. The particles interacting in the first, second and third cell, prior to the intersection point, were summed. The percentages of total particles interacting prior to the intersection point were ratioed to 100% and are listed in Table 9.

Table 9. Percent of initial particles to interact prior to intersection point.

MeV	% Particles Between 2' and 3'	% Particles to Reach Intersection	% Particles weighted to 100%
1	0.69	0.0112%	48.71%
2	0.71	0.0083%	36.32%
3	0.75	0.0015%	6.59%
5	0.76	0.0008%	3.64%
7.5	0.77	0.0007%	2.91%
10	0.77	0.0004%	1.83%

The monoenergetic photon energy simulations were only an energy estimation starting point, and it was understood that the photons produced from the core would have a distribution of energies. The percentages listed in Table 9 were determined to help define the photon source spectral shape.

5.2 Exposure Rates – Energy Distributions

The first simulation using an energy distribution, simulation 8, was run with source photon energy percentages as listed in Table 9. The measured exposure values and calculated exposure values of simulation 8 are presented in Table 10.

Table 10. Source activity and calculated exposure of simulation 8.

Position Above Core (ft)	Source Activity (γ/hr)	Calculated Exposure Rate (R/hr)	Measured Exposure Rate (R/hr)
0	4.3211E+16 ± 1.39E+15	1000 ± 100	1000 ± 100
1		180 ± 100	360 ± 100
2		47 ± 10	72 ± 10
3		10.8 ± 1	10 ± 1
4		1.46 ± 0.1	2 ± 0.1
5		0.46 ± 0.01	0.4 ± 0.01
16		0.00 ± 0.01	

A plot of the calculated versus measured exposure with corresponding errors is shown in Figure 17. The exposures rates in the ion chamber positions 3 ft and higher are within the error limits for the measured exposure. Simulations 9 through 11 were then run with varied percentages to attempt a closer match to the measure exposure values. However, simulation 8 most closely matched the measured exposure rates.

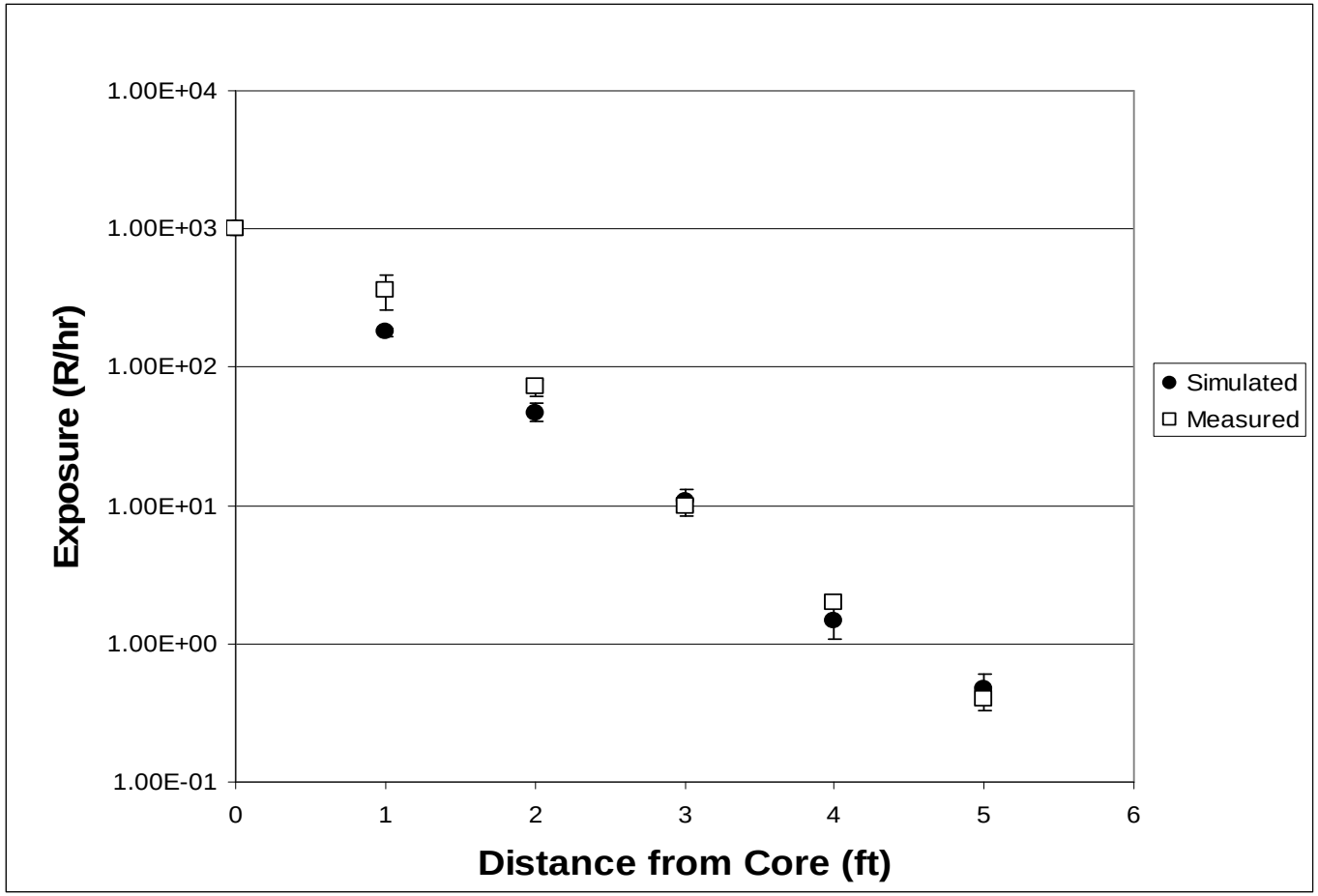

Figure 17. Exposure rates (R/hr) from simulation 8 and measured values at various heights above the TRIGA reactor core.

5.3 Dose Calculation at the Reactor Top

After approximating the photon energy distribution, MCNP5 was run with all primary water surrounding the core removed. Equation 18 was rearranged to solve for the dose rate at the reactor top using the *F8 tally from the MCNP5. The activity was the source activity from simulation 8. The exposure rates as a function of height above the core 7 hours after shutdown are given in Table 11.

Table 11. Simulated exposure levels for a LOCA at positions above the reactor core.

Position	Source Activity (γ/Hour)	R/hr (Calculated)	MCNP Mev/Initial Photon
Top of core	4.3211E+16 ± 1.39E+15	2212 ± 53	1.1078E-05 ± 2.669798E-07
1 ft above core		839 ± 31	4.2002E-06 ± 1.558270E-07
2 ft above core		429 ± 23	2.1492E-06 ± 1.126165E-07
3 ft above core		276 ± 18	1.3812E-06 ± 9.184914E-08
4 ft above core		187 ± 14	9.3516E-07 ± 7.023029E-08
5 ft above core		159 ± 14	7.9514E-07 ± 7.124472E-08
Reactor Top		10 ± 2	5.0351E-08 ± 1.194319E-08

The source activity was then converted to curies and compared to the activity calculated with Equation 7. A plot of the activity versus time is shown in Figure 18. The individual data point is the activity at the reactor top determined from MCNP5 7 hours after shutdown. The time gap of 7 hours was used because the initial exposure measurements were taken 7 hours after the reactor was shutdown. The exposure measurements were taken prior to the beginning of this project, and the gap of 7 hours was outside of the scope of control for this project.

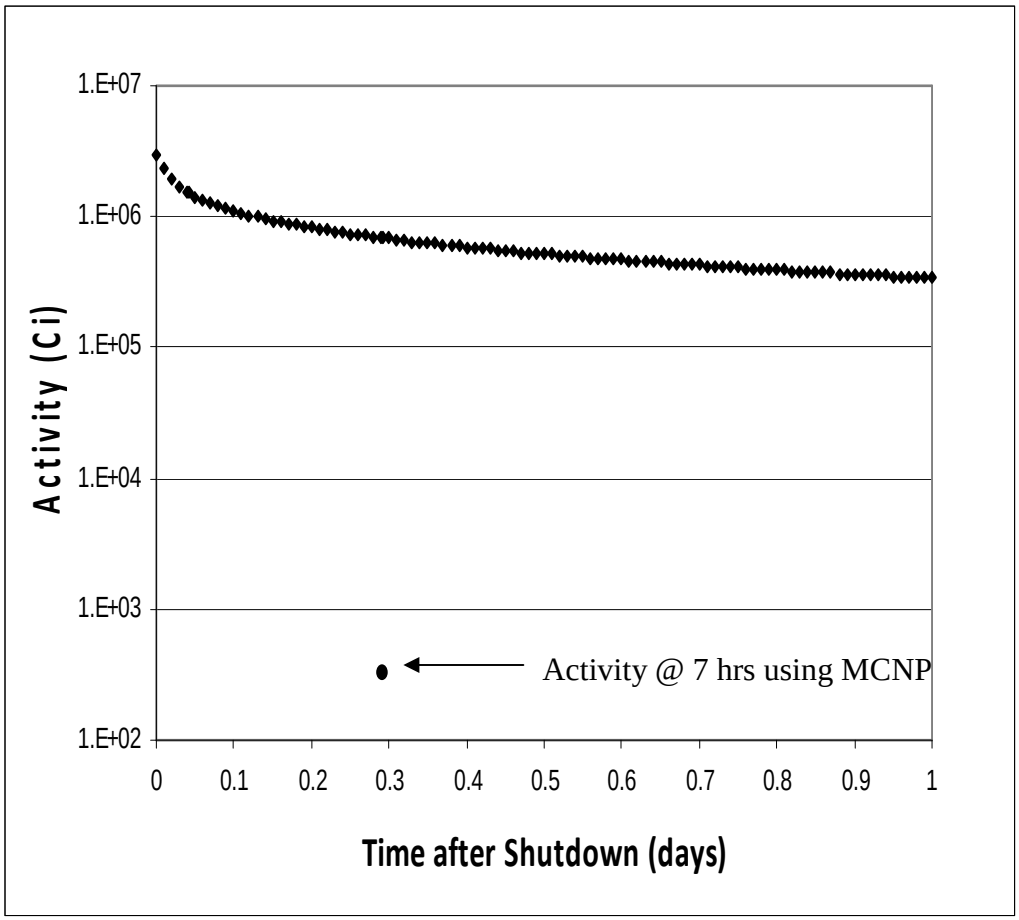

Figure 18. Fission product activity as a function of time after shutdown with activity calculated using Equation 7.

The activity estimated from MCNP5 is less than the activity estimated from core exposure measurements and equation 7. The MCNP5 model significantly underestimates source activity because it only accounted for decays which emitted photons but not other types of emitted radiation. The reactor operating time in equation 7 was adjusted to account for the discrepancy, effectively shifting the curve in Figure 18 so that the individual data point of activity lies on the curve.

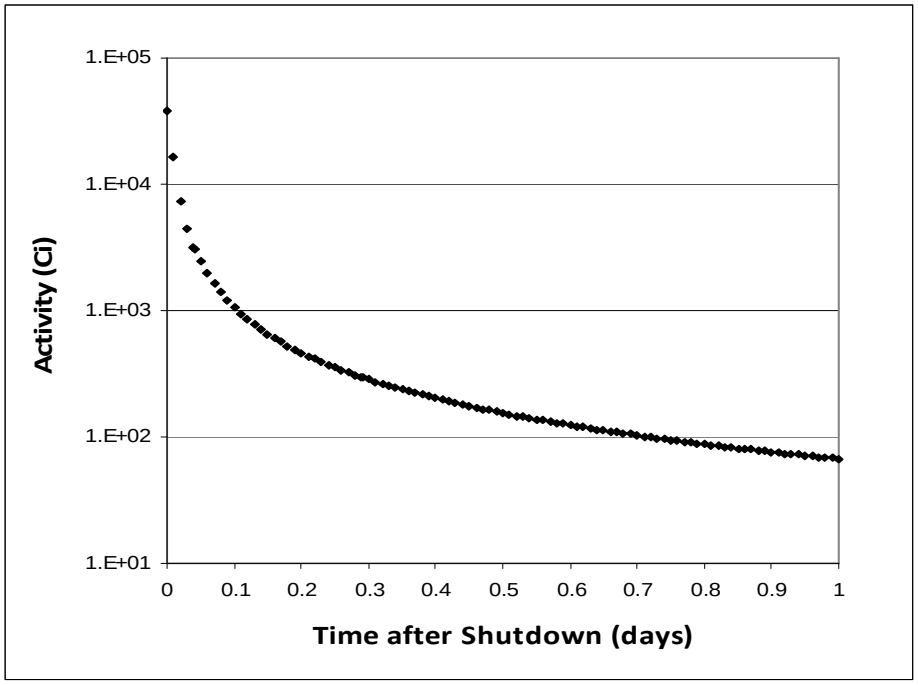

Figure 19. Corrected fission product activity.

At time zero, the activity of the core was estimated at 3.79×10^4 Ci, or 5.05×10^{18} photons per hour. Using this activity, exposure rates were calculated at times after shutdown, and are displayed in Table 12. .

The differences in the activity determined from MCNP5 verses the activity using equation 7 are due to several assumptions used for the equation. First, the MCNP5 model assumes the only radiation energy depositing in the cells is from photons. Equation 7 takes into account radioactive decay produced from all radiation; therefore decays that result in alpha and neutron radiation would be absent from the MCNP5 model. MCNP5 does track the electrons created during the photon interactions and, for the photon only mode, deposits their energy at the point of the photon interaction. Secondly, the TRIGA reactor operation is cyclic with start ups and shutdowns throughout the year on an almost daily basis. The cyclic operation will result in a buildup of longer lived isotopes over a period of time, while

allowing time for the shorter lived isotopes to decay away. This cyclic operation is not accounted for in equation 7.

Using activity values from Figure 19, the exposure was calculated for various times after shutdown. Using equation 13, exposure rate was converted to dose rate and a weighting factor of 1 for photons was used to convert dose rate to dose equivalent rate. The results are compared with the OSTR SAR predicted dose equivalent rates in Table 12.

Table 12. Exposure and dose rates after LOCA at the top of the TRIGA® bioshield.

Time	Source Activity (γ/Hour)	Exposure Rate (R/hr)	Dose Rate (rad/hr)	Dose Equivalent Rate (rem/hr)	Dose Equivalent Rate from SAR (rem/hr)
0	5.055E+18	1031	904	904	1.00E+04
1 hr	4.041E+17	82	72	72	1.52E+03
1 day	8.947E+15	2	2	2	1.19E+03
1 week	8.662E+14	0.18	0.2	0.2	6.39E+02
1 month	1.511E+14	0.03	0.03	0.03	3.51E+02

5.4 Facility External Dose

Dose rates external to the reactor building are given in Figure 20. The figure displays the maximum dose rate, for each 1 meter width increment, on the east side of the reactor building. The range of interest extends from the OSTR east wall up to 60 meters in the horizontal direction. The horizontal blocks, shown in Figure 21, demonstrate an aerial view of the 5 rows of cells that of were modeled from 0 to 100 cm in the z-axis direction (height) east of the reactor facility. Each block contained 60 of the 1 meter in width and height cells.

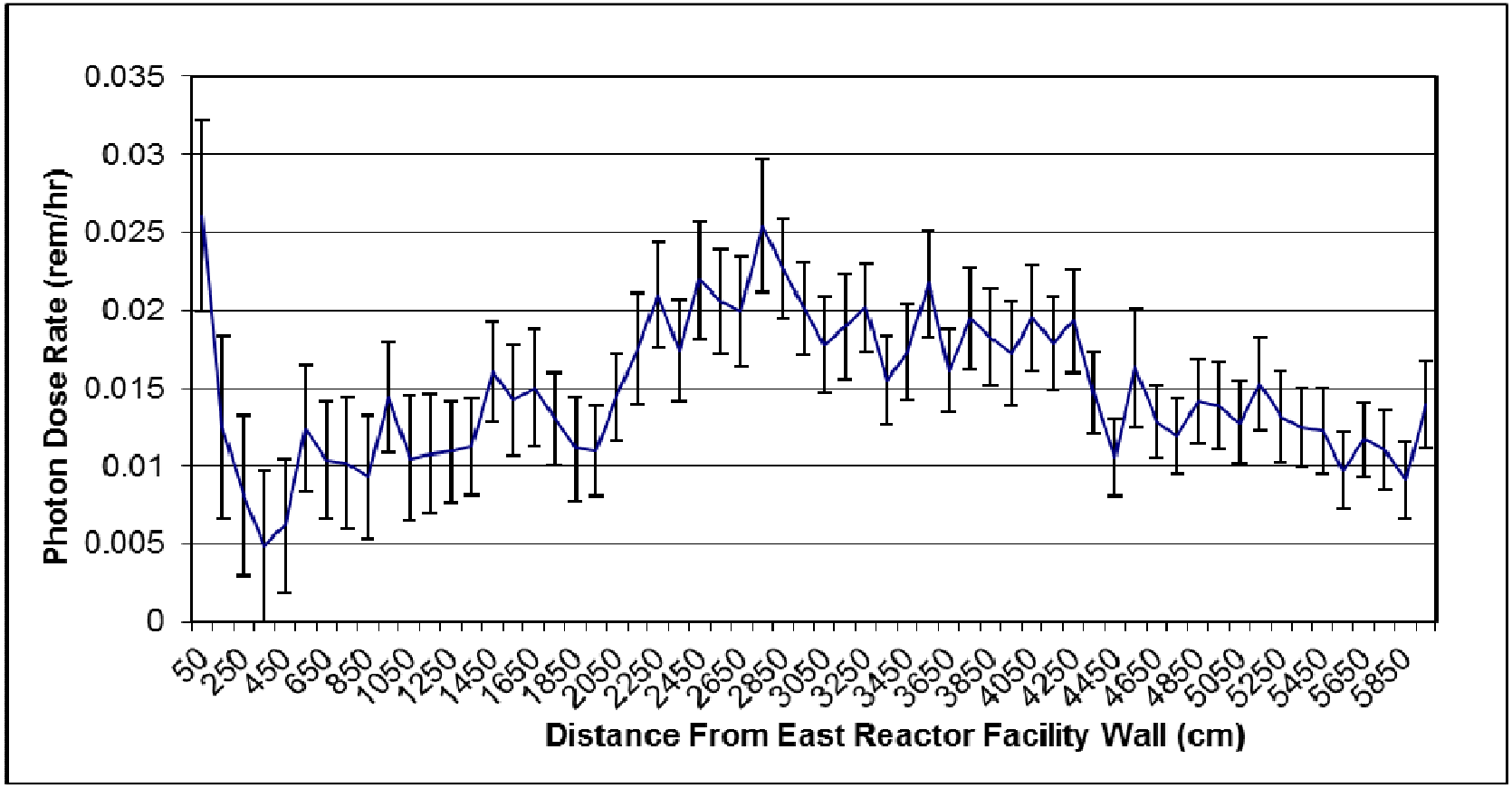

Figure 20. Dose rates external to OSTR from 0 to 100 cm in height.

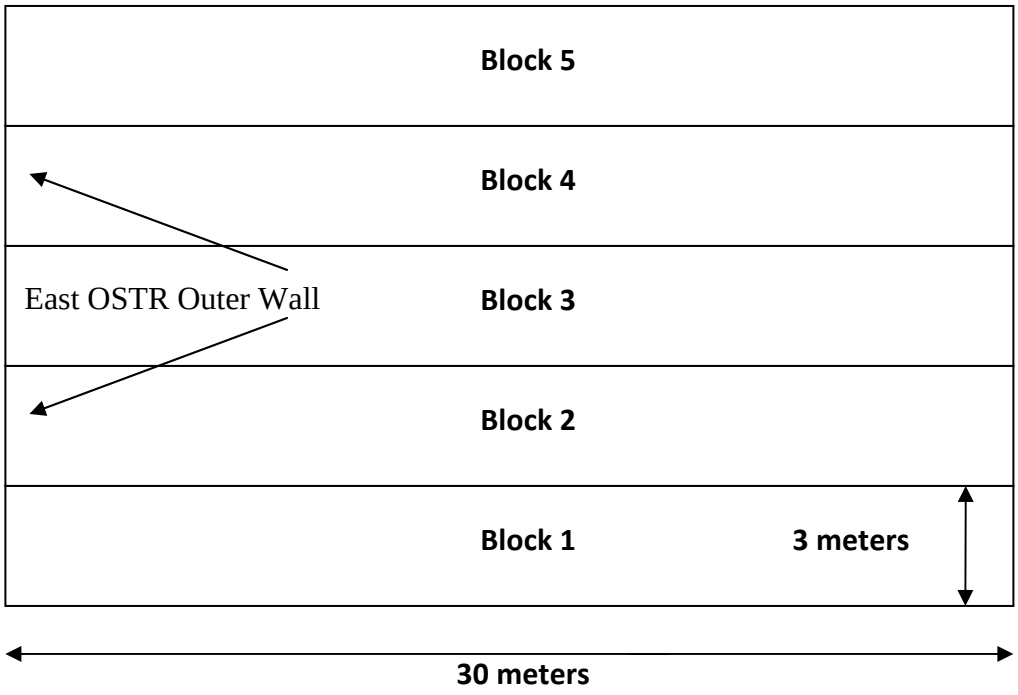

Figure 21. Cell positions for photon dose rates in Figure 19.

Dose rates on the OSTR exterior peak at approximately 30 mrem/hr. The dose rates calculated assume an activity equivalent to the activity present exactly at the end of bombardment.

To determine the dose received within the first hour after a LOCA event, equation 7 was integrated from time 0 hr to time 1 hr after shutdown. The operating time used was 0.00239923 days, which corresponds to the operating time required to match the MCNP5 modeled core activity. The dose within the first hour is 5.33E-3 mrem using the integrated activity from equation 15.

6 Conclusion

This thesis presented an approach to estimate dose rates due to photon skyshine on the exterior of the OSTR building in the event of a LOCA. The findings presented herein indicate that the dose rates of a cell 1 meter in

height may meet the NRC limit of 2 mrem/hr in the event of a LOCA at the OSTR. The dose rates at the reactor top were estimated to be less than the values calculated in the OSTR SAR. However, a direct comparison for the skyshine is not available from the OSTR SAR. The OSTR SAR only takes into account scatter from the reactor building ceiling, and not scatter due to skyshine from the atmosphere above the reactor building. However, the source strength initially used for dose rate calculations would be the same, so one may assume that an overestimation of dose rates at the facility perimeter would also occur.

There are two reasons why the results presented here do not match the OSTR SAR. First, the OSTR SAR assumes that the reactor has been operating continuously for the previous 365 days. This assumption will cause a higher value to be calculated for the activity using equation 7. In reality the reactor operates on a cyclic schedule, and the short lived isotopes have time to decay prior to the next start up. This reduction in short lived isotopes would reduce the activity estimated at shut down, which is consistent with the results obtained from this analysis. Secondly, the SAR assumes only monoenergetic photons of 1 MeV from the source. This is most likely an inaccurate assumption and affects the energy distribution seen at heights above the core.

6.1 Future Work

The analysis presented for this thesis provides validation that the equations used in the OSTR SAR may be overestimating dose rates external to the radiation facility. Future work could involve the determination of a correction factor to be used in conjunction with the methods displayed in the OSTR SAR. A correction factor would provide less conservative, yet likely more accurate dose rates.

BIBLIOGRAPHY

[1] "Subpart D--Radiation Dose Limits for Individual Members of the Public". Nuclear Regulator Commission. 4/26/2010 <http://www.nrc.gov/reading-rm/doc-collections/cfr/part020/part020-1301.html>.

[2] U.S. Department of Energy, "The Manhattan Project". Office of History & Heritage Resources.5/7/2009 <http://www.cfo.doe.gov/me70/manhattan/cp-1_critical.htm>.

[3] Teller, Edward, and Judith Schoolery. Memoirs: A Twentieth-Century Journey in Science and Politics. Cambridge: Perseus Books Group, 2001.

[4] General Atomics. "TRIGA Research Reactors". General Atomics. 4/15/2010 <http://www.gaesi.com/triga/about/index.php>.

[5] Radiation Center: Irradiation Facilities". Oregon State University. 2/15/2010 <http://radiationcenter.oregonstate.edu/Irrad%20Facilities/Facilities%20home.html>.

[6] Anderson, T.V., *Oregon State TRIGA Reactor Training Manual*. 1990.

[7] Lewis, Elmer E.. Fundamentals of Nuclear Reactor Physics. San Diego: Elsevier Inc., 2008.

[8] "Appendix A to Part 50--General Design Criteria for Nuclear Power Plants". Nuclear Regulator Commission. 4/26/2010 <http://www.nrc.gov/reading-rm/doc-collections/cfr/part050/part050-appa.html>.

[9] *Safety Analysis Report for the Oregon State University TRIGA Reactor*. Rev. 0, 2004. Print

[10] Lamarsh, John R. Introduction to Nuclear Engineering, 3rd Edition . New Jersey: Prentice Hall, 2001.

[11] *Safety Analysis Report for the UC Davis TRIGA Reactor*. Print.

[12] McGinley, Patton H. “Radiation Skyshine Produced by an 18 MeV Medical Accelerator.” *Radiation Protection Management,* Vol 10 No. 5, 1993. pp. 59-64.

[13] National Council on Radiation Protection and Measurements, Radiation protection design guidelines for 0.1-100 MeV particle accelerator facilities. Washington, D.C.: NCRP; NCRP Report No. 51; 1977.

[14] US Department of Energy, DOE FUNDAMENTALS HANDBOOK NUCLEAR PHYSICS AND REACTOR THEORY. 2 vols. Washington D.C.: Department of Energy, 1993.

[15] Martin, James E. Physics for Radiation Protection, a Handbook, 2nd ed. Germany: Wiley-VCH, 2006.

[16] Lilley, John. Nuclear Physics: Principles and Applications. Hoboken: John Wiley & Sons, Inc., 2001.

[17] Knoll, Glenn F. Radiation Detection and Measurement,3rd ed. Hoboken: Wiley, 2000.

[18] Lagunita, I.S., et al.. "Skyshine from photon radiation". Atomic Energy February, 1989: 118-124.

[19] X-5 Monte Carlo Team, MCNP - A General Monte Carlo N-Particle Transport Code, Version 5. 3 vols. Los Alamos , 2003.

[20] *Non-Routine (Special) Radiation Survey Record*. Corvallis, Oregon: Oregon State University Radiation Center, 1999. Print.

APPENDICES

A APPENDIX – MCNP5 INPUT FOR LOCA SIMULATION

```
TRIGA REACTOR
c cell definitions
1 1 -3.12 1 -2 3 -4 5 -6 13 $Bioshield Base
2 3 -.0012 6 -2 3 -4 5 -12 13 $Second Layer Bioshield
3 1 -3.12 12 -11 -2 3 -4 5 13 $Third Layer Bioshield
4 3 -.0012 1 -11 22 4 -28 -24 $Room Air North
5 3 -.0012 1 -11 26 -5 22 -24 $Room Air South
6 3 -.0012 1 -11 -24 2 -4 5 $Room Air East
7 3 -.0012 1 -11 -14 22 -4 5 $Room Air West (West PIF)
8 3 -.0012 1 -33 -4 17 -3 14 $Room Air West (North PIF)
9 3 -.0012 1 -33 -19 5 -3 14 $Room Air West (South PIF)
10 3 -.0012 -11 33 14 -3 -4 5 $Room Air West (Top PIF)
11 3 -.0012 11 -30 3 -2 -28 26 $Room Air Top - Middle
12 3 -.0012 11 -30 -3 22 -28 26 $Room Air Top - West
13 3 -.0012 11 -30 2 -24 -28 26 $Room Air Top - East
14 1 -3.12 1 -30 24 -25 26 -28 $East Wall
15 1 -3.12 1 -30 -22 23 26 -28 $West Wall
16 1 -3.12 1 -30 -29 28 23 -25 $North Wall
17 1 -3.12 1 -30 -26 27 23 -25 $South Wall
18 4 -8.0 30 -31 23 -25 -29 27 $Ceiling
c 19 0 -1:31:-23:25:-27:29 $Void
20 1 -3.12 1 -11 -13 32 $Cylinder Cement
c 21 0 1 -32 -11 $Cylinder Void
22 1 -3.12 1 -33 14 -21 -17 19 $West Wall - PIF
23 1 -3.12 1 -33 -17 18 21 -16 $North Wall - PIF
24 1 -3.12 1 -33 -17 19 -3 16 $East Wall - PIF
25 1 -3.12 1 -33 -20 19 -16 21 $South wall - PIF
26 2 -1 1 -33 -18 20 -16 21 $PIF Water
27 3 -.0012 1 -31 -36 37 -34 78 $North Field Outside Reactor
28 3 -.0012 1 -31 -36 37 -67 35 $South Field Outside Reactor
c 29 3 -.0012 1 -31 -29 27 -36 134 $East Field Outside Reactor
30 3 -.0012 1 -31 -29 27 -55 37 $West Field Outside Reactor
c 31 3 -.0012 31 -38 -34 35 -36 37 $Air Above Reactor Building
32 0 -1:38:34:-35:36:-37 $Void outside of Fields
33 3 -.0012 1 -11 -32 39 $Water outside of core cylinder volume (lateral only)
34 3 -.0012 1 -40 -39 $Outside portion of core cylinder (water below core)
35 2 -1 40 -41 -39 $Outside portion of core cylinder (core material)
36 3 -.0012 41 -52 53 -39 $Water above core, outside test air cylinders (Water, Bottom)
c 37 2 -1 1 -40 -53 $Inside portion of core cylinder (water below core)
c 38 2 -19.05 40 -41 -53 $Inside portion of core cylinder (Core Material)
39 3 -.0012 41 -42 -53 $Inside portion of core cylinder - Air TEST 1
40 3 -.0012 42 -43 -53 $Inside portion of core cylinder - Water 1'
41 3 -.0012 43 -44 -53 $Inside portion of core cylinder - Air TEST 2
42 3 -.0012 44 -45 -53 $Inside portion of core cylinder - Water 2'
43 3 -.0012 45 -46 -53 $Inside portion of core cylinder - Air TEST 3
44 3 -.0012 46 -47 -53 $Inside portion of core cylinder - Water 3'
45 3 -.0012 47 -48 -53 $Inside portion of core cylinder - Air TEST 4
46 3 -.0012 48 -49 -53 $Inside portion of core cylinder - Water 4'
47 3 -.0012 49 -50 -53 $Inside portion of core cylinder - Air TEST 5
48 3 -.0012 50 -51 -53 $Inside portion of core cylinder - Water 5'
49 3 -.0012 51 -52 -53 $Inside portion of core cylinder - Air Test 6
50 3 -.0012 52 -54 -53 $Inside portion of core cylinder - Water 6'
51 3 -.0012 52 -11 53 -39 $ Water Above core, outside test air cylinders (Top)
52 3 -.0012 54 -11 -53 $Top most air test cylinder
c cells external to facility for dose calculations
53 3 -.0012 1 -31 55 -56 67 -68
54 3 -.0012 1 -31 56 -57 67 -68
55 3 -.0012 1 -31 57 -58 67 -68
56 3 -.0012 1 -31 58 -23 67 -68
```

57 3 -.0012 1 -31 23 -59 67 -68
58 3 -.0012 1 -31 59 -60 67 -68
59 3 -.0012 1 -31 60 -61 67 -68
60 3 -.0012 1 -31 61 -62 67 -68
61 3 -.0012 1 -31 62 -25 67 -68
62 3 -.0012 1 -31 25 -63 67 -68
63 3 -.0012 1 -31 63 -64 67 -68
64 3 -.0012 1 -31 64 -65 67 -68
65 3 -.0012 1 -31 65 -66 67 -68
66 3 -.0012 1 -31 55 -56 68 -69
67 3 -.0012 1 -31 56 -57 68 -69
68 3 -.0012 1 -31 57 -58 68 -69
69 3 -.0012 1 -31 58 -23 68 -69
70 3 -.0012 1 -31 23 -59 68 -69
71 3 -.0012 1 -31 59 -60 68 -69
72 3 -.0012 1 -31 60 -61 68 -69
73 3 -.0012 1 -31 61 -62 68 -69
74 3 -.0012 1 -31 62 -25 68 -69
75 3 -.0012 1 -31 25 -63 68 -69
76 3 -.0012 1 -31 63 -64 68 -69
77 3 -.0012 1 -31 64 -65 68 -69
78 3 -.0012 1 -31 65 -66 68 -69
79 3 -.0012 1 -31 55 -56 69 -70
80 3 -.0012 1 -31 56 -57 69 -70
81 3 -.0012 1 -31 57 -58 69 -70
82 3 -.0012 1 -31 58 -23 69 -70
83 3 -.0012 1 -31 23 -59 69 -70
84 3 -.0012 1 -31 59 -60 69 -70
85 3 -.0012 1 -31 60 -61 69 -70
86 3 -.0012 1 -31 61 -62 69 -70
87 3 -.0012 1 -31 62 -25 69 -70
88 3 -.0012 1 -31 25 -63 69 -70
89 3 -.0012 1 -31 63 -64 69 -70
90 3 -.0012 1 -31 64 -65 69 -70
91 3 -.0012 1 -31 65 -66 69 -70
92 3 -.0012 1 -31 55 -56 70 -27
93 3 -.0012 1 -31 56 -57 70 -27
94 3 -.0012 1 -31 57 -58 70 -27
95 3 -.0012 1 -31 58 -23 70 -27
96 3 -.0012 1 -31 23 -59 70 -27
97 3 -.0012 1 -31 59 -60 70 -27
98 3 -.0012 1 -31 60 -61 70 -27
99 3 -.0012 1 -31 61 -62 70 -27
100 3 -.0012 1 -31 62 -25 70 -27
101 3 -.0012 1 -31 25 -63 70 -27
102 3 -.0012 1 -31 63 -64 70 -27
103 3 -.0012 1 -31 64 -65 70 -27
104 3 -.0012 1 -31 65 -66 70 -27
105 3 -.0012 1 -31 55 -56 27 -71
106 3 -.0012 1 -31 56 -57 27 -71
107 3 -.0012 1 -31 57 -58 27 -71
108 3 -.0012 1 -31 58 -23 27 -71
109 3 -.0012 1 -31 55 -56 71 -72
110 3 -.0012 1 -31 56 -57 71 -72
111 3 -.0012 1 -31 57 -58 71 -72
112 3 -.0012 1 -31 58 -23 71 -72
113 3 -.0012 1 -31 55 -56 72 -73
114 3 -.0012 1 -31 56 -57 72 -73
115 3 -.0012 1 -31 57 -58 72 -73
116 3 -.0012 1 -31 58 -23 72 -73
117 3 -.0012 1 -31 55 -56 73 -74

118 3 -.0012 1 -31 56 -57 73 -74
119 3 -.0012 1 -31 57 -58 73 -74
120 3 -.0012 1 -31 58 -23 73 -74
121 3 -.0012 1 -31 55 -56 74 -29
122 3 -.0012 1 -31 56 -57 74 -29
123 3 -.0012 1 -31 57 -58 74 -29
124 3 -.0012 1 -31 58 -23 74 -29
c 125 3 -.0012 1 -31 25 -63 27 -71
c 126 3 -.0012 1 -31 63 -64 27 -71
c 127 3 -.0012 1 -31 64 -65 27 -71
c 128 3 -.0012 1 -31 65 -66 27 -71
c 129 3 -.0012 1 -31 25 -63 71 -72
c 130 3 -.0012 1 -31 63 -64 71 -72
c 131 3 -.0012 1 -31 64 -65 71 -72
c 132 3 -.0012 1 -31 65 -66 71 -72
c 133 3 -.0012 1 -31 25 -63 72 -73
c 134 3 -.0012 1 -31 63 -64 72 -73
c 135 3 -.0012 1 -31 64 -65 72 -73
c 136 3 -.0012 1 -31 65 -66 72 -73
c 137 3 -.0012 1 -31 25 -63 73 -74
c 138 3 -.0012 1 -31 63 -64 73 -74
c 139 3 -.0012 1 -31 64 -65 73 -74
c 140 3 -.0012 1 -31 65 -66 73 -74
c 141 3 -.0012 1 -31 25 -63 74 -29
c 142 3 -.0012 1 -31 63 -64 74 -29
c 143 3 -.0012 1 -31 64 -65 74 -29
c 144 3 -.0012 1 -31 65 -66 74 -29
145 3 -.0012 1 -31 55 -56 29 -75
146 3 -.0012 1 -31 56 -57 29 -75
147 3 -.0012 1 -31 57 -58 29 -75
148 3 -.0012 1 -31 58 -23 29 -75
149 3 -.0012 1 -31 23 -59 29 -75
150 3 -.0012 1 -31 59 -60 29 -75
151 3 -.0012 1 -31 60 -61 29 -75
152 3 -.0012 1 -31 61 -62 29 -75
153 3 -.0012 1 -31 62 -25 29 -75
154 3 -.0012 1 -31 25 -63 29 -75
155 3 -.0012 1 -31 63 -64 29 -75
156 3 -.0012 1 -31 64 -65 29 -75
157 3 -.0012 1 -31 65 -66 29 -75
158 3 -.0012 1 -31 55 -56 75 -76
159 3 -.0012 1 -31 56 -57 75 -76
160 3 -.0012 1 -31 57 -58 75 -76
161 3 -.0012 1 -31 58 -23 75 -76
162 3 -.0012 1 -31 23 -59 75 -76
163 3 -.0012 1 -31 59 -60 75 -76
164 3 -.0012 1 -31 60 -61 75 -76
165 3 -.0012 1 -31 61 -62 75 -76
166 3 -.0012 1 -31 62 -25 75 -76
167 3 -.0012 1 -31 25 -63 75 -76
168 3 -.0012 1 -31 63 -64 75 -76
169 3 -.0012 1 -31 64 -65 75 -76
170 3 -.0012 1 -31 65 -66 75 -76
171 3 -.0012 1 -31 55 -56 76 -77
172 3 -.0012 1 -31 56 -57 76 -77
173 3 -.0012 1 -31 57 -58 76 -77
174 3 -.0012 1 -31 58 -23 76 -77
175 3 -.0012 1 -31 23 -59 76 -77
176 3 -.0012 1 -31 59 -60 76 -77
177 3 -.0012 1 -31 60 -61 76 -77
178 3 -.0012 1 -31 61 -62 76 -77

179 3 -.0012 1 -31 62 -25 76 -77
180 3 -.0012 1 -31 25 -63 76 -77
181 3 -.0012 1 -31 63 -64 76 -77
182 3 -.0012 1 -31 64 -65 76 -77
183 3 -.0012 1 -31 65 -66 76 -77
184 3 -.0012 1 -31 55 -56 77 -78
185 3 -.0012 1 -31 56 -57 77 -78
186 3 -.0012 1 -31 57 -58 77 -78
187 3 -.0012 1 -31 58 -23 77 -78
188 3 -.0012 1 -31 23 -59 77 -78
189 3 -.0012 1 -31 59 -60 77 -78
190 3 -.0012 1 -31 60 -61 77 -78
191 3 -.0012 1 -31 61 -62 77 -78
192 3 -.0012 1 -31 62 -25 77 -78
193 3 -.0012 1 -31 25 -63 77 -78
194 3 -.0012 1 -31 63 -64 77 -78
195 3 -.0012 1 -31 64 -65 77 -78
196 3 -.0012 1 -31 65 -66 77 -78
197 3 -.0012 1 -31 37 -55 29 -78
198 3 -.0012 1 -31 66 -36 29 -78
199 3 -.0012 1 -31 37 -55 67 -27
200 3 -.0012 1 -31 66 -36 67 -27
201 3 -0.0012 1 -98 25 -79 27 -71
202 3 -0.0012 98 -31 25 -79 27 -71
203 3 -0.0012 1 -98 25 -79 71 -72
204 3 -0.0012 98 -31 25 -79 71 -72
205 3 -0.0012 1 -98 25 -79 72 -73
206 3 -0.0012 98 -31 25 -79 72 -73
207 3 -0.0012 1 -98 25 -79 73 -74
208 3 -0.0012 98 -31 25 -79 73 -74
209 3 -0.0012 1 -98 25 -79 74 -29
210 3 -0.0012 98 -31 25 -79 74 -29
211 3 -0.0012 1 -98 79 -80 27 -71
212 3 -0.0012 98 -31 79 -80 27 -71
213 3 -0.0012 1 -98 79 -80 71 -72
214 3 -0.0012 98 -31 79 -80 71 -72
215 3 -0.0012 1 -98 79 -80 72 -73
216 3 -0.0012 98 -31 79 -80 72 -73
217 3 -0.0012 1 -98 79 -80 73 -74
218 3 -0.0012 98 -31 79 -80 73 -74
219 3 -0.0012 1 -98 79 -80 74 -29
220 3 -0.0012 98 -31 79 -80 74 -29
221 3 -0.0012 1 -98 80 -63 27 -71
222 3 -0.0012 98 -31 80 -63 27 -71
223 3 -0.0012 1 -98 80 -63 71 -72
224 3 -0.0012 98 -31 80 -63 71 -72
225 3 -0.0012 1 -98 80 -63 72 -73
226 3 -0.0012 98 -31 80 -63 72 -73
227 3 -0.0012 1 -98 80 -63 73 -74
228 3 -0.0012 98 -31 80 -63 73 -74
229 3 -0.0012 1 -98 80 -63 74 -29
230 3 -0.0012 98 -31 80 -63 74 -29
231 3 -0.0012 1 -98 63 -81 27 -71
232 3 -0.0012 98 -31 63 -81 27 -71
233 3 -0.0012 1 -98 63 -81 71 -72
234 3 -0.0012 98 -31 63 -81 71 -72
235 3 -0.0012 1 -98 63 -81 72 -73
236 3 -0.0012 98 -31 63 -81 72 -73
237 3 -0.0012 1 -98 63 -81 73 -74
238 3 -0.0012 98 -31 63 -81 73 -74
239 3 -0.0012 1 -98 63 -81 74 -29

240 3 -0.0012 98 -31 63 -81 74 -29
241 3 -0.0012 1 -98 81 -82 27 -71
242 3 -0.0012 98 -31 81 -82 27 -71
243 3 -0.0012 1 -98 81 -82 71 -72
244 3 -0.0012 98 -31 81 -82 71 -72
245 3 -0.0012 1 -98 81 -82 72 -73
246 3 -0.0012 98 -31 81 -82 72 -73
247 3 -0.0012 1 -98 81 -82 73 -74
248 3 -0.0012 98 -31 81 -82 73 -74
249 3 -0.0012 1 -98 81 -82 74 -29
250 3 -0.0012 98 -31 81 -82 74 -29
251 3 -0.0012 1 -98 82 -64 27 -71
252 3 -0.0012 98 -31 82 -64 27 -71
253 3 -0.0012 1 -98 82 -64 71 -72
254 3 -0.0012 98 -31 82 -64 71 -72
255 3 -0.0012 1 -98 82 -64 72 -73
256 3 -0.0012 98 -31 82 -64 72 -73
257 3 -0.0012 1 -98 82 -64 73 -74
258 3 -0.0012 98 -31 82 -64 73 -74
259 3 -0.0012 1 -98 82 -64 74 -29
260 3 -0.0012 98 -31 82 -64 74 -29
261 3 -0.0012 1 -98 64 -83 27 -71
262 3 -0.0012 98 -31 64 -83 27 -71
263 3 -0.0012 1 -98 64 -83 71 -72
264 3 -0.0012 98 -31 64 -83 71 -72
265 3 -0.0012 1 -98 64 -83 72 -73
266 3 -0.0012 98 -31 64 -83 72 -73
267 3 -0.0012 1 -98 64 -83 73 -74
268 3 -0.0012 98 -31 64 -83 73 -74
269 3 -0.0012 1 -98 64 -83 74 -29
270 3 -0.0012 98 -31 64 -83 74 -29
271 3 -0.0012 1 -98 83 -84 27 -71
272 3 -0.0012 98 -31 83 -84 27 -71
273 3 -0.0012 1 -98 83 -84 71 -72
274 3 -0.0012 98 -31 83 -84 71 -72
275 3 -0.0012 1 -98 83 -84 72 -73
276 3 -0.0012 98 -31 83 -84 72 -73
277 3 -0.0012 1 -98 83 -84 73 -74
278 3 -0.0012 98 -31 83 -84 73 -74
279 3 -0.0012 1 -98 83 -84 74 -29
280 3 -0.0012 98 -31 83 -84 74 -29
281 3 -0.0012 1 -98 84 -65 27 -71
282 3 -0.0012 98 -31 84 -65 27 -71
283 3 -0.0012 1 -98 84 -65 71 -72
284 3 -0.0012 98 -31 84 -65 71 -72
285 3 -0.0012 1 -98 84 -65 72 -73
286 3 -0.0012 98 -31 84 -65 72 -73
287 3 -0.0012 1 -98 84 -65 73 -74
288 3 -0.0012 98 -31 84 -65 73 -74
289 3 -0.0012 1 -98 84 -65 74 -29
290 3 -0.0012 98 -31 84 -65 74 -29
291 3 -0.0012 1 -98 65 -85 27 -71
292 3 -0.0012 98 -31 65 -85 27 -71
293 3 -0.0012 1 -98 65 -85 71 -72
294 3 -0.0012 98 -31 65 -85 71 -72
295 3 -0.0012 1 -98 65 -85 72 -73
296 3 -0.0012 98 -31 65 -85 72 -73
297 3 -0.0012 1 -98 65 -85 73 -74
298 3 -0.0012 98 -31 65 -85 73 -74
299 3 -0.0012 1 -98 65 -85 74 -29
300 3 -0.0012 98 -31 65 -85 74 -29

301 3 -0.0012 1 -98 85 -86 27 -71
302 3 -0.0012 98 -31 85 -86 27 -71
303 3 -0.0012 1 -98 85 -86 71 -72
304 3 -0.0012 98 -31 85 -86 71 -72
305 3 -0.0012 1 -98 85 -86 72 -73
306 3 -0.0012 98 -31 85 -86 72 -73
307 3 -0.0012 1 -98 85 -86 73 -74
308 3 -0.0012 98 -31 85 -86 73 -74
309 3 -0.0012 1 -98 85 -86 74 -29
310 3 -0.0012 98 -31 85 -86 74 -29
311 3 -0.0012 1 -98 86 -66 27 -71
312 3 -0.0012 98 -31 86 -66 27 -71
313 3 -0.0012 1 -98 86 -66 71 -72
314 3 -0.0012 98 -31 86 -66 71 -72
315 3 -0.0012 1 -98 86 -66 72 -73
316 3 -0.0012 98 -31 86 -66 72 -73
317 3 -0.0012 1 -98 86 -66 73 -74
318 3 -0.0012 98 -31 86 -66 73 -74
319 3 -0.0012 1 -98 86 -66 74 -29
320 3 -0.0012 98 -31 86 -66 74 -29
321 3 -0.0012 1 -98 66 -87 27 -71
322 3 -0.0012 98 -31 66 -87 27 -71
323 3 -0.0012 1 -98 66 -87 71 -72
324 3 -0.0012 98 -31 66 -87 71 -72
325 3 -0.0012 1 -98 66 -87 72 -73
326 3 -0.0012 98 -31 66 -87 72 -73
327 3 -0.0012 1 -98 66 -87 73 -74
328 3 -0.0012 98 -31 66 -87 73 -74
329 3 -0.0012 1 -98 66 -87 74 -29
330 3 -0.0012 98 -31 66 -87 74 -29
331 3 -0.0012 1 -98 87 -88 27 -71
332 3 -0.0012 98 -31 87 -88 27 -71
333 3 -0.0012 1 -98 87 -88 71 -72
334 3 -0.0012 98 -31 87 -88 71 -72
335 3 -0.0012 1 -98 87 -88 72 -73
336 3 -0.0012 98 -31 87 -88 72 -73
337 3 -0.0012 1 -98 87 -88 73 -74
338 3 -0.0012 98 -31 87 -88 73 -74
339 3 -0.0012 1 -98 87 -88 74 -29
340 3 -0.0012 98 -31 87 -88 74 -29
341 3 -0.0012 1 -98 88 -89 27 -71
342 3 -0.0012 98 -31 88 -89 27 -71
343 3 -0.0012 1 -98 88 -89 71 -72
344 3 -0.0012 98 -31 88 -89 71 -72
345 3 -0.0012 1 -98 88 -89 72 -73
346 3 -0.0012 98 -31 88 -89 72 -73
347 3 -0.0012 1 -98 88 -89 73 -74
348 3 -0.0012 98 -31 88 -89 73 -74
349 3 -0.0012 1 -98 88 -89 74 -29
350 3 -0.0012 98 -31 88 -89 74 -29
351 3 -0.0012 1 -98 89 -90 27 -71
352 3 -0.0012 98 -31 89 -90 27 -71
353 3 -0.0012 1 -98 89 -90 71 -72
354 3 -0.0012 98 -31 89 -90 71 -72
355 3 -0.0012 1 -98 89 -90 72 -73
356 3 -0.0012 98 -31 89 -90 72 -73
357 3 -0.0012 1 -98 89 -90 73 -74
358 3 -0.0012 98 -31 89 -90 73 -74
359 3 -0.0012 1 -98 89 -90 74 -29
360 3 -0.0012 98 -31 89 -90 74 -29
361 3 -0.0012 1 -98 90 -91 27 -71

362 3 -0.0012 98 -31 90 -91 27 -71
363 3 -0.0012 1 -98 90 -91 71 -72
364 3 -0.0012 98 -31 90 -91 71 -72
365 3 -0.0012 1 -98 90 -91 72 -73
366 3 -0.0012 98 -31 90 -91 72 -73
367 3 -0.0012 1 -98 90 -91 73 -74
368 3 -0.0012 98 -31 90 -91 73 -74
369 3 -0.0012 1 -98 90 -91 74 -29
370 3 -0.0012 98 -31 90 -91 74 -29
371 3 -0.0012 1 -98 91 -92 27 -71
372 3 -0.0012 98 -31 91 -92 27 -71
373 3 -0.0012 1 -98 91 -92 71 -72
374 3 -0.0012 98 -31 91 -92 71 -72
375 3 -0.0012 1 -98 91 -92 72 -73
376 3 -0.0012 98 -31 91 -92 72 -73
377 3 -0.0012 1 -98 91 -92 73 -74
378 3 -0.0012 98 -31 91 -92 73 -74
379 3 -0.0012 1 -98 91 -92 74 -29
380 3 -0.0012 98 -31 91 -92 74 -29
381 3 -0.0012 1 -98 92 -93 27 -71
382 3 -0.0012 98 -31 92 -93 27 -71
383 3 -0.0012 1 -98 92 -93 71 -72
384 3 -0.0012 98 -31 92 -93 71 -72
385 3 -0.0012 1 -98 92 -93 72 -73
386 3 -0.0012 98 -31 92 -93 72 -73
387 3 -0.0012 1 -98 92 -93 73 -74
388 3 -0.0012 98 -31 92 -93 73 -74
389 3 -0.0012 1 -98 92 -93 74 -29
390 3 -0.0012 98 -31 92 -93 74 -29
391 3 -0.0012 1 -98 93 -94 27 -71
392 3 -0.0012 98 -31 93 -94 27 -71
393 3 -0.0012 1 -98 93 -94 71 -72
394 3 -0.0012 98 -31 93 -94 71 -72
395 3 -0.0012 1 -98 93 -94 72 -73
396 3 -0.0012 98 -31 93 -94 72 -73
397 3 -0.0012 1 -98 93 -94 73 -74
398 3 -0.0012 98 -31 93 -94 73 -74
399 3 -0.0012 1 -98 93 -94 74 -29
400 3 -0.0012 98 -31 93 -94 74 -29
401 3 -0.0012 1 -98 94 -95 27 -71
402 3 -0.0012 98 -31 94 -95 27 -71
403 3 -0.0012 1 -98 94 -95 71 -72
404 3 -0.0012 98 -31 94 -95 71 -72
405 3 -0.0012 1 -98 94 -95 72 -73
406 3 -0.0012 98 -31 94 -95 72 -73
407 3 -0.0012 1 -98 94 -95 73 -74
408 3 -0.0012 98 -31 94 -95 73 -74
409 3 -0.0012 1 -98 94 -95 74 -29
410 3 -0.0012 98 -31 94 -95 74 -29
411 3 -0.0012 1 -98 95 -96 27 -71
412 3 -0.0012 98 -31 95 -96 27 -71
413 3 -0.0012 1 -98 95 -96 71 -72
414 3 -0.0012 98 -31 95 -96 71 -72
415 3 -0.0012 1 -98 95 -96 72 -73
416 3 -0.0012 98 -31 95 -96 72 -73
417 3 -0.0012 1 -98 95 -96 73 -74
418 3 -0.0012 98 -31 95 -96 73 -74
419 3 -0.0012 1 -98 95 -96 74 -29
420 3 -0.0012 98 -31 95 -96 74 -29
421 3 -0.0012 1 -98 96 -97 27 -71
422 3 -0.0012 98 -31 96 -97 27 -71

423 3 -0.0012 1 -98 96 -97 71 -72
424 3 -0.0012 98 -31 96 -97 71 -72
425 3 -0.0012 1 -98 96 -97 72 -73
426 3 -0.0012 98 -31 96 -97 72 -73
427 3 -0.0012 1 -98 96 -97 73 -74
428 3 -0.0012 98 -31 96 -97 73 -74
429 3 -0.0012 1 -98 96 -97 74 -29
430 3 -0.0012 98 -31 96 -97 74 -29
431 3 -.0012 31 -38 37 35 -34 -23
432 3 -.0012 31 -38 35 23 -27 -25
433 3 -.0012 31 -38 27 -29 23 -25
434 3 -.0012 31 -38 29 -34 23 -25
435 3 -.0012 31 -38 29 -34 25 -36
436 3 -.0012 31 -38 25 -36 -29 27
437 3 -.0012 31 -38 35 -27 25 -36
438 3 -0.0012 1 -98 27 -71 97 -99
439 3 -0.0012 98 -31 27 -71 97 -99
440 3 -0.0012 1 -98 71 -72 97 -99
441 3 -0.0012 98 -31 71 -72 97 -99
442 3 -0.0012 1 -98 72 -73 97 -99
443 3 -0.0012 98 -31 72 -73 97 -99
444 3 -0.0012 1 -98 73 -74 97 -99
445 3 -0.0012 98 -31 73 -74 97 -99
446 3 -0.0012 1 -98 74 -29 97 -99
447 3 -0.0012 98 -31 74 -29 97 -99
448 3 -0.0012 1 -98 27 -71 99 -100
449 3 -0.0012 98 -31 27 -71 99 -100
450 3 -0.0012 1 -98 71 -72 99 -100
451 3 -0.0012 98 -31 71 -72 99 -100
452 3 -0.0012 1 -98 72 -73 99 -100
453 3 -0.0012 98 -31 72 -73 99 -100
454 3 -0.0012 1 -98 73 -74 99 -100
455 3 -0.0012 98 -31 73 -74 99 -100
456 3 -0.0012 1 -98 74 -29 99 -100
457 3 -0.0012 98 -31 74 -29 99 -100
458 3 -0.0012 1 -98 27 -71 100 -101
459 3 -0.0012 98 -31 27 -71 100 -101
460 3 -0.0012 1 -98 71 -72 100 -101
461 3 -0.0012 98 -31 71 -72 100 -101
462 3 -0.0012 1 -98 72 -73 100 -101
463 3 -0.0012 98 -31 72 -73 100 -101
464 3 -0.0012 1 -98 73 -74 100 -101
465 3 -0.0012 98 -31 73 -74 100 -101
466 3 -0.0012 1 -98 74 -29 100 -101
467 3 -0.0012 98 -31 74 -29 100 -101
468 3 -0.0012 1 -98 27 -71 101 -102
469 3 -0.0012 98 -31 27 -71 101 -102
470 3 -0.0012 1 -98 71 -72 101 -102
471 3 -0.0012 98 -31 71 -72 101 -102
472 3 -0.0012 1 -98 72 -73 101 -102
473 3 -0.0012 98 -31 72 -73 101 -102
474 3 -0.0012 1 -98 73 -74 101 -102
475 3 -0.0012 98 -31 73 -74 101 -102
476 3 -0.0012 1 -98 74 -29 101 -102
477 3 -0.0012 98 -31 74 -29 101 -102
478 3 -0.0012 1 -98 27 -71 102 -103
479 3 -0.0012 98 -31 27 -71 102 -103
480 3 -0.0012 1 -98 71 -72 102 -103
481 3 -0.0012 98 -31 71 -72 102 -103
482 3 -0.0012 1 -98 72 -73 102 -103
483 3 -0.0012 98 -31 72 -73 102 -103

484 3 -0.0012 1 -98 73 -74 102 -103
485 3 -0.0012 98 -31 73 -74 102 -103
486 3 -0.0012 1 -98 74 -29 102 -103
487 3 -0.0012 98 -31 74 -29 102 -103
488 3 -0.0012 1 -98 27 -71 103 -104
489 3 -0.0012 98 -31 27 -71 103 -104
490 3 -0.0012 1 -98 71 -72 103 -104
491 3 -0.0012 98 -31 71 -72 103 -104
492 3 -0.0012 1 -98 72 -73 103 -104
493 3 -0.0012 98 -31 72 -73 103 -104
494 3 -0.0012 1 -98 73 -74 103 -104
495 3 -0.0012 98 -31 73 -74 103 -104
496 3 -0.0012 1 -98 74 -29 103 -104
497 3 -0.0012 98 -31 74 -29 103 -104
498 3 -0.0012 1 -98 27 -71 104 -105
499 3 -0.0012 98 -31 27 -71 104 -105
500 3 -0.0012 1 -98 71 -72 104 -105
501 3 -0.0012 98 -31 71 -72 104 -105
502 3 -0.0012 1 -98 72 -73 104 -105
503 3 -0.0012 98 -31 72 -73 104 -105
504 3 -0.0012 1 -98 73 -74 104 -105
505 3 -0.0012 98 -31 73 -74 104 -105
506 3 -0.0012 1 -98 74 -29 104 -105
507 3 -0.0012 98 -31 74 -29 104 -105
508 3 -0.0012 1 -98 27 -71 105 -106
509 3 -0.0012 98 -31 27 -71 105 -106
510 3 -0.0012 1 -98 71 -72 105 -106
511 3 -0.0012 98 -31 71 -72 105 -106
512 3 -0.0012 1 -98 72 -73 105 -106
513 3 -0.0012 98 -31 72 -73 105 -106
514 3 -0.0012 1 -98 73 -74 105 -106
515 3 -0.0012 98 -31 73 -74 105 -106
516 3 -0.0012 1 -98 74 -29 105 -106
517 3 -0.0012 98 -31 74 -29 105 -106
518 3 -0.0012 1 -98 27 -71 106 -107
519 3 -0.0012 98 -31 27 -71 106 -107
520 3 -0.0012 1 -98 71 -72 106 -107
521 3 -0.0012 98 -31 71 -72 106 -107
522 3 -0.0012 1 -98 72 -73 106 -107
523 3 -0.0012 98 -31 72 -73 106 -107
524 3 -0.0012 1 -98 73 -74 106 -107
525 3 -0.0012 98 -31 73 -74 106 -107
526 3 -0.0012 1 -98 74 -29 106 -107
527 3 -0.0012 98 -31 74 -29 106 -107
528 3 -0.0012 1 -98 27 -71 107 -108
529 3 -0.0012 98 -31 27 -71 107 -108
530 3 -0.0012 1 -98 71 -72 107 -108
531 3 -0.0012 98 -31 71 -72 107 -108
532 3 -0.0012 1 -98 72 -73 107 -108
533 3 -0.0012 98 -31 72 -73 107 -108
534 3 -0.0012 1 -98 73 -74 107 -108
535 3 -0.0012 98 -31 73 -74 107 -108
536 3 -0.0012 1 -98 74 -29 107 -108
537 3 -0.0012 98 -31 74 -29 107 -108
538 3 -0.0012 1 -98 27 -71 108 -109
539 3 -0.0012 98 -31 27 -71 108 -109
540 3 -0.0012 1 -98 71 -72 108 -109
541 3 -0.0012 98 -31 71 -72 108 -109
542 3 -0.0012 1 -98 72 -73 108 -109
543 3 -0.0012 98 -31 72 -73 108 -109
544 3 -0.0012 1 -98 73 -74 108 -109

545 3 -0.0012 98 -31 73 -74 108 -109
546 3 -0.0012 1 -98 74 -29 108 -109
547 3 -0.0012 98 -31 74 -29 108 -109
548 3 -0.0012 1 -98 27 -71 109 -110
549 3 -0.0012 98 -31 27 -71 109 -110
550 3 -0.0012 1 -98 71 -72 109 -110
551 3 -0.0012 98 -31 71 -72 109 -110
552 3 -0.0012 1 -98 72 -73 109 -110
553 3 -0.0012 98 -31 72 -73 109 -110
554 3 -0.0012 1 -98 73 -74 109 -110
555 3 -0.0012 98 -31 73 -74 109 -110
556 3 -0.0012 1 -98 74 -29 109 -110
557 3 -0.0012 98 -31 74 -29 109 -110
558 3 -0.0012 1 -98 27 -71 110 -111
559 3 -0.0012 98 -31 27 -71 110 -111
560 3 -0.0012 1 -98 71 -72 110 -111
561 3 -0.0012 98 -31 71 -72 110 -111
562 3 -0.0012 1 -98 72 -73 110 -111
563 3 -0.0012 98 -31 72 -73 110 -111
564 3 -0.0012 1 -98 73 -74 110 -111
565 3 -0.0012 98 -31 73 -74 110 -111
566 3 -0.0012 1 -98 74 -29 110 -111
567 3 -0.0012 98 -31 74 -29 110 -111
568 3 -0.0012 1 -98 27 -71 111 -112
569 3 -0.0012 98 -31 27 -71 111 -112
570 3 -0.0012 1 -98 71 -72 111 -112
571 3 -0.0012 98 -31 71 -72 111 -112
572 3 -0.0012 1 -98 72 -73 111 -112
573 3 -0.0012 98 -31 72 -73 111 -112
574 3 -0.0012 1 -98 73 -74 111 -112
575 3 -0.0012 98 -31 73 -74 111 -112
576 3 -0.0012 1 -98 74 -29 111 -112
577 3 -0.0012 98 -31 74 -29 111 -112
578 3 -0.0012 1 -98 27 -71 112 -113
579 3 -0.0012 98 -31 27 -71 112 -113
580 3 -0.0012 1 -98 71 -72 112 -113
581 3 -0.0012 98 -31 71 -72 112 -113
582 3 -0.0012 1 -98 72 -73 112 -113
583 3 -0.0012 98 -31 72 -73 112 -113
584 3 -0.0012 1 -98 73 -74 112 -113
585 3 -0.0012 98 -31 73 -74 112 -113
586 3 -0.0012 1 -98 74 -29 112 -113
587 3 -0.0012 98 -31 74 -29 112 -113
588 3 -0.0012 1 -98 27 -71 113 -114
589 3 -0.0012 98 -31 27 -71 113 -114
590 3 -0.0012 1 -98 71 -72 113 -114
591 3 -0.0012 98 -31 71 -72 113 -114
592 3 -0.0012 1 -98 72 -73 113 -114
593 3 -0.0012 98 -31 72 -73 113 -114
594 3 -0.0012 1 -98 73 -74 113 -114
595 3 -0.0012 98 -31 73 -74 113 -114
596 3 -0.0012 1 -98 74 -29 113 -114
597 3 -0.0012 98 -31 74 -29 113 -114
598 3 -0.0012 1 -98 27 -71 114 -115
599 3 -0.0012 98 -31 27 -71 114 -115
600 3 -0.0012 1 -98 71 -72 114 -115
601 3 -0.0012 98 -31 71 -72 114 -115
602 3 -0.0012 1 -98 72 -73 114 -115
603 3 -0.0012 98 -31 72 -73 114 -115
604 3 -0.0012 1 -98 73 -74 114 -115
605 3 -0.0012 98 -31 73 -74 114 -115

606 3 -0.0012 1 -98 74 -29 114 -115
607 3 -0.0012 98 -31 74 -29 114 -115
608 3 -0.0012 1 -98 27 -71 115 -116
609 3 -0.0012 98 -31 27 -71 115 -116
610 3 -0.0012 1 -98 71 -72 115 -116
611 3 -0.0012 98 -31 71 -72 115 -116
612 3 -0.0012 1 -98 72 -73 115 -116
613 3 -0.0012 98 -31 72 -73 115 -116
614 3 -0.0012 1 -98 73 -74 115 -116
615 3 -0.0012 98 -31 73 -74 115 -116
616 3 -0.0012 1 -98 74 -29 115 -116
617 3 -0.0012 98 -31 74 -29 115 -116
618 3 -0.0012 1 -98 27 -71 116 -117
619 3 -0.0012 98 -31 27 -71 116 -117
620 3 -0.0012 1 -98 71 -72 116 -117
621 3 -0.0012 98 -31 71 -72 116 -117
622 3 -0.0012 1 -98 72 -73 116 -117
623 3 -0.0012 98 -31 72 -73 116 -117
624 3 -0.0012 1 -98 73 -74 116 -117
625 3 -0.0012 98 -31 73 -74 116 -117
626 3 -0.0012 1 -98 74 -29 116 -117
627 3 -0.0012 98 -31 74 -29 116 -117
628 3 -0.0012 1 -98 27 -71 117 -118
629 3 -0.0012 98 -31 27 -71 117 -118
630 3 -0.0012 1 -98 71 -72 117 -118
631 3 -0.0012 98 -31 71 -72 117 -118
632 3 -0.0012 1 -98 72 -73 117 -118
633 3 -0.0012 98 -31 72 -73 117 -118
634 3 -0.0012 1 -98 73 -74 117 -118
635 3 -0.0012 98 -31 73 -74 117 -118
636 3 -0.0012 1 -98 74 -29 117 -118
637 3 -0.0012 98 -31 74 -29 117 -118
638 3 -0.0012 1 -98 27 -71 118 -119
639 3 -0.0012 98 -31 27 -71 118 -119
640 3 -0.0012 1 -98 71 -72 118 -119
641 3 -0.0012 98 -31 71 -72 118 -119
642 3 -0.0012 1 -98 72 -73 118 -119
643 3 -0.0012 98 -31 72 -73 118 -119
644 3 -0.0012 1 -98 73 -74 118 -119
645 3 -0.0012 98 -31 73 -74 118 -119
646 3 -0.0012 1 -98 74 -29 118 -119
647 3 -0.0012 98 -31 74 -29 118 -119
648 3 -0.0012 1 -98 27 -71 119 -120
649 3 -0.0012 98 -31 27 -71 119 -120
650 3 -0.0012 1 -98 71 -72 119 -120
651 3 -0.0012 98 -31 71 -72 119 -120
652 3 -0.0012 1 -98 72 -73 119 -120
653 3 -0.0012 98 -31 72 -73 119 -120
654 3 -0.0012 1 -98 73 -74 119 -120
655 3 -0.0012 98 -31 73 -74 119 -120
656 3 -0.0012 1 -98 74 -29 119 -120
657 3 -0.0012 98 -31 74 -29 119 -120
658 3 -0.0012 1 -98 27 -71 120 -121
659 3 -0.0012 98 -31 27 -71 120 -121
660 3 -0.0012 1 -98 71 -72 120 -121
661 3 -0.0012 98 -31 71 -72 120 -121
662 3 -0.0012 1 -98 72 -73 120 -121
663 3 -0.0012 98 -31 72 -73 120 -121
664 3 -0.0012 1 -98 73 -74 120 -121
665 3 -0.0012 98 -31 73 -74 120 -121
666 3 -0.0012 1 -98 74 -29 120 -121

667 3 -0.0012 98 -31 74 -29 120 -121
668 3 -0.0012 1 -98 27 -71 121 -122
669 3 -0.0012 98 -31 27 -71 121 -122
670 3 -0.0012 1 -98 71 -72 121 -122
671 3 -0.0012 98 -31 71 -72 121 -122
672 3 -0.0012 1 -98 72 -73 121 -122
673 3 -0.0012 98 -31 72 -73 121 -122
674 3 -0.0012 1 -98 73 -74 121 -122
675 3 -0.0012 98 -31 73 -74 121 -122
676 3 -0.0012 1 -98 74 -29 121 -122
677 3 -0.0012 98 -31 74 -29 121 -122
678 3 -0.0012 1 -98 27 -71 122 -123
679 3 -0.0012 98 -31 27 -71 122 -123
680 3 -0.0012 1 -98 71 -72 122 -123
681 3 -0.0012 98 -31 71 -72 122 -123
682 3 -0.0012 1 -98 72 -73 122 -123
683 3 -0.0012 98 -31 72 -73 122 -123
684 3 -0.0012 1 -98 73 -74 122 -123
685 3 -0.0012 98 -31 73 -74 122 -123
686 3 -0.0012 1 -98 74 -29 122 -123
687 3 -0.0012 98 -31 74 -29 122 -123
688 3 -0.0012 1 -98 27 -71 123 -124
689 3 -0.0012 98 -31 27 -71 123 -124
690 3 -0.0012 1 -98 71 -72 123 -124
691 3 -0.0012 98 -31 71 -72 123 -124
692 3 -0.0012 1 -98 72 -73 123 -124
693 3 -0.0012 98 -31 72 -73 123 -124
694 3 -0.0012 1 -98 73 -74 123 -124
695 3 -0.0012 98 -31 73 -74 123 -124
696 3 -0.0012 1 -98 74 -29 123 -124
697 3 -0.0012 98 -31 74 -29 123 -124
698 3 -0.0012 1 -98 27 -71 124 -125
699 3 -0.0012 98 -31 27 -71 124 -125
700 3 -0.0012 1 -98 71 -72 124 -125
701 3 -0.0012 98 -31 71 -72 124 -125
702 3 -0.0012 1 -98 72 -73 124 -125
703 3 -0.0012 98 -31 72 -73 124 -125
704 3 -0.0012 1 -98 73 -74 124 -125
705 3 -0.0012 98 -31 73 -74 124 -125
706 3 -0.0012 1 -98 74 -29 124 -125
707 3 -0.0012 98 -31 74 -29 124 -125
708 3 -0.0012 1 -98 27 -71 125 -126
709 3 -0.0012 98 -31 27 -71 125 -126
710 3 -0.0012 1 -98 71 -72 125 -126
711 3 -0.0012 98 -31 71 -72 125 -126
712 3 -0.0012 1 -98 72 -73 125 -126
713 3 -0.0012 98 -31 72 -73 125 -126
714 3 -0.0012 1 -98 73 -74 125 -126
715 3 -0.0012 98 -31 73 -74 125 -126
716 3 -0.0012 1 -98 74 -29 125 -126
717 3 -0.0012 98 -31 74 -29 125 -126
718 3 -0.0012 1 -98 27 -71 126 -127
719 3 -0.0012 98 -31 27 -71 126 -127
720 3 -0.0012 1 -98 71 -72 126 -127
721 3 -0.0012 98 -31 71 -72 126 -127
722 3 -0.0012 1 -98 72 -73 126 -127
723 3 -0.0012 98 -31 72 -73 126 -127
724 3 -0.0012 1 -98 73 -74 126 -127
725 3 -0.0012 98 -31 73 -74 126 -127
726 3 -0.0012 1 -98 74 -29 126 -127
727 3 -0.0012 98 -31 74 -29 126 -127

728 3 -0.0012 1 -98 27 -71 127 -128
729 3 -0.0012 98 -31 27 -71 127 -128
730 3 -0.0012 1 -98 71 -72 127 -128
731 3 -0.0012 98 -31 71 -72 127 -128
732 3 -0.0012 1 -98 72 -73 127 -128
733 3 -0.0012 98 -31 72 -73 127 -128
734 3 -0.0012 1 -98 73 -74 127 -128
735 3 -0.0012 98 -31 73 -74 127 -128
736 3 -0.0012 1 -98 74 -29 127 -128
737 3 -0.0012 98 -31 74 -29 127 -128
738 3 -0.0012 1 -98 27 -71 128 -129
739 3 -0.0012 98 -31 27 -71 128 -129
740 3 -0.0012 1 -98 71 -72 128 -129
741 3 -0.0012 98 -31 71 -72 128 -129
742 3 -0.0012 1 -98 72 -73 128 -129
743 3 -0.0012 98 -31 72 -73 128 -129
744 3 -0.0012 1 -98 73 -74 128 -129
745 3 -0.0012 98 -31 73 -74 128 -129
746 3 -0.0012 1 -98 74 -29 128 -129
747 3 -0.0012 98 -31 74 -29 128 -129
748 3 -0.0012 1 -98 27 -71 129 -130
749 3 -0.0012 98 -31 27 -71 129 -130
750 3 -0.0012 1 -98 71 -72 129 -130
751 3 -0.0012 98 -31 71 -72 129 -130
752 3 -0.0012 1 -98 72 -73 129 -130
753 3 -0.0012 98 -31 72 -73 129 -130
754 3 -0.0012 1 -98 73 -74 129 -130
755 3 -0.0012 98 -31 73 -74 129 -130
756 3 -0.0012 1 -98 74 -29 129 -130
757 3 -0.0012 98 -31 74 -29 129 -130
758 3 -0.0012 1 -98 27 -71 130 -131
759 3 -0.0012 98 -31 27 -71 130 -131
760 3 -0.0012 1 -98 71 -72 130 -131
761 3 -0.0012 98 -31 71 -72 130 -131
762 3 -0.0012 1 -98 72 -73 130 -131
763 3 -0.0012 98 -31 72 -73 130 -131
764 3 -0.0012 1 -98 73 -74 130 -131
765 3 -0.0012 98 -31 73 -74 130 -131
766 3 -0.0012 1 -98 74 -29 130 -131
767 3 -0.0012 98 -31 74 -29 130 -131
768 3 -0.0012 1 -98 27 -71 131 -132
769 3 -0.0012 98 -31 27 -71 131 -132
770 3 -0.0012 1 -98 71 -72 131 -132
771 3 -0.0012 98 -31 71 -72 131 -132
772 3 -0.0012 1 -98 72 -73 131 -132
773 3 -0.0012 98 -31 72 -73 131 -132
774 3 -0.0012 1 -98 73 -74 131 -132
775 3 -0.0012 98 -31 73 -74 131 -132
776 3 -0.0012 1 -98 74 -29 131 -132
777 3 -0.0012 98 -31 74 -29 131 -132
778 3 -0.0012 1 -98 27 -71 132 -133
779 3 -0.0012 98 -31 27 -71 132 -133
780 3 -0.0012 1 -98 71 -72 132 -133
781 3 -0.0012 98 -31 71 -72 132 -133
782 3 -0.0012 1 -98 72 -73 132 -133
783 3 -0.0012 98 -31 72 -73 132 -133
784 3 -0.0012 1 -98 73 -74 132 -133
785 3 -0.0012 98 -31 73 -74 132 -133
786 3 -0.0012 1 -98 74 -29 132 -133
787 3 -0.0012 98 -31 74 -29 132 -133
788 3 -0.0012 1 -98 27 -71 133 -134

```
789 3 -0.0012 98 -31 27 -71 133 -134
790 3 -0.0012 1 -98 71 -72 133 -134
791 3 -0.0012 98 -31 71 -72 133 -134
792 3 -0.0012 1 -98 72 -73 133 -134
793 3 -0.0012 98 -31 72 -73 133 -134
794 3 -0.0012 1 -98 73 -74 133 -134
795 3 -0.0012 98 -31 73 -74 133 -134
796 3 -0.0012 1 -98 74 -29 133 -134
797 3 -0.0012 98 -31 74 -29 133 -134
798 3 -0.0012 1 -98 27 -71 134 -36
799 3 -0.0012 98 -31 27 -71 134 -36
800 3 -0.0012 1 -98 71 -72 134 -36
801 3 -0.0012 98 -31 71 -72 134 -36
802 3 -0.0012 1 -98 72 -73 134 -36
803 3 -0.0012 98 -31 72 -73 134 -36
804 3 -0.0012 1 -98 73 -74 134 -36
805 3 -0.0012 98 -31 73 -74 134 -36
806 3 -0.0012 1 -98 74 -29 134 -36
807 3 -0.0012 98 -31 74 -29 134 -36

c Surface Definitions
1 pz 0 $Bioshield Base
2 px 347.98 $East Bioshield Base
3 px -190.5 $West Bioshield Base
4 py 346.63  $North Bioshield Base
5 py -346.63  $South Bioshield Base
6 pz 369.718  $Bioshield Base top
c 7 1 py 346.63  $North East Corner, Transformation 1
c 8 2 py 346.63  $North West Corner, Transformation 2
c 9 3 py -346.63 $South East Corner, Transformation 3
c 10 4 py -346.63 $South West Corner, Transformation 4
11 pz 739.436  $Top of Reactor
12 pz 655.32 $Top of Cylinder (middle layer)
13 cz 190.5 $Reactor Bioshield Cylinder
14 px -515.62  $West outside wall PIF
16 px -290.5  $East inside wall PIF
17 py 246.63  $North outside wall PIF
18 py 146.63  $North inside wall PIF
19 py -246.63  $South outside wall PIF
20 py -146.63  $South inside wall PIF
21 px -415.63  $West inside wall PIF
22 px -759.46  $West Inside Wall
23 px -779.78  $West Outside Wall
24 px 1221.7  $East Inside Wall
25 px 1242.1  $East Outside Wall
26 py -836.85  $South Inside Wall
27 py -857.17  $South Outside Wall
28 py 836.85  $North Inside Wall
29 py 857.17  $North Outside Wall
30 pz 944.88  $Ceiling Bottom - Stainless Steel
31 pz 945.198  $Ceiling Top
32 cz 99.06 $Inside Bioshield Cylinder
33 pz 365.76 $PIF TOP
34 py 5240 $North Outside Field
35 py -5240 $South Outside Field
36 px 7242.1 $East Outside Field
37 px -5240 $West Outside Field
38 pz 1500 $Top most plane of air above reactor building.
39 cz 63.5 $Core Cylinder
40 pz 91.44 $Bottom plane for core cylinder
41 pz 144.78 $Top plane for core cylinder
```

```
42 pz 154.94 $Top plane 1st Air Cylinder
43 pz 175.26 $Bottom plane for 2nd air cylinder
44 pz 185.42 $Top plane for 2nd air cylinder
45 pz 205.74 $Bottom plane for 3rd air cylinder
46 pz 215.90 $Top plane for 3rd air cylinder
47 pz 236.22 $Bottom plane for 4th air cylinder
48 pz 246.38 $Top plane for 4th air cylinder
49 pz 261.62 $Bottom plane for 5th air cylinder
50 pz 271.78 $Top plane for 5th air cylinder
51 pz 292.10 $Bottom plane for 6th air cylinder
52 pz 302.26 $Top plane for 6th air cylinder
53 cz 10.16 $Air Test Cylinder
54 pz 729.276 $Air cylinder top of core cylinder
55 px -1979.78
56 px -1679.78
57 px -1379.78
58 px -1079.78
59 px -375.4
60 px 28.98
61 px 433.36
62 px 837.74
63 px 1542.1
64 px 1842.1
65 px 2142.1
66 px 2442.1
67 py -2057.17
68 py -1757.17
69 py -1457.17
70 py -1157.17
71 py -514.3
72 py -171.43
73 py 171.43
74 py 514.3
75 py 1157.17
76 py 1457.17
77 py 1757.17
78 py 2057.17
79 px 1342.1
80 px 1442.1
81 px 1642.1
82 px 1742.2
83 px 1942.1
84 px 2042.1
85 px 2242.1
86 px 2342.1
87 px 2542.1
88 px 2642.1
89 px 2742.1
90 px 2842.1
91 px 2942.1
92 px 3042.1
93 px 3142.1
94 px 3242.1
95 px 3342.1
96 px 3442.1
97 px 3542.1
98 pz 100 $Plane to split external cells into sections up to 1 meter, then above 1 meter
99 px 3642.1
100 px 3742.1
101 px 3842.1
102 px 3942.1
```

```
103 px 4042.1
104 px 4142.1
105 px 4242.1
106 px 4342.1
107 px 4442.1
108 px 4542.1
109 px 4642.1
110 px 4742.1
111 px 4842.1
112 px 4942.1
113 px 5042.1
114 px 5142.1
115 px 5242.1
116 px 5342.1
117 px 5442.1
118 px 5542.1
119 px 5642.1
120 px 5742.1
121 px 5842.1
122 px 5942.1
123 px 6042.1
124 px 6142.1
125 px 6242.1
126 px 6342.1
127 px 6442.1
128 px 6542.1
129 px 6642.1
130 px 6742.1
131 px 6842.1
132 px 6942.1
133 px 7042.1
134 px 7142.1

c Material Definitions
mode p
m1   020040     43.5  $ Calcium Cement (atom ratio)
     008016     77.6  $ Oxygen
     014028     14.1  $ Si
     013027     3.04   $ Al
     026056     1    $ Fe
m2   001001      2  $Water (H)
     008016     1  $Water (O)
m3   015031      3  $Air (N)
     008016     1  $Air (O)
m4   026056     70 $Iron
     006012     8  $Carbon
     024052     18 $Chromium
     025055     1  $Manganese
     014028     1  $Silicon
     015030     1  $Phosphorus
     016032     1  $Sulfur
sdef ERG=D1 POS=0 0 144 AXS=0 0 1 CELL=35 RAD=D2 VEC=0 0 1 DIR=1
sI1 H 0 1 2 3 5 7.5 10 $particle distribution
sP1 D 0 0.692329 0.2492384 0.0498477 0.0069233 0.0013847 0.0002769
SI2 64
*f8:p 39 41 43 45 47 49 52 201 202 203 204 205 206 207 208 209 210 211 212
     213 214 215 216 217 218 219 220 221 222 223 224 225 226 227 228 229
     230 231 232 233 234 235 236 237 238 239 240 241 242 243 244 245 246
     247 248 249 250 251 252 253 254 255 256 257 258 259 260 261 262 263
     264 265 266 267 268 269 270 271 272 273 274 275 276 277 278 279 280
     281 282 283 284 285 286 287 288 289 290 291 292 293 294 295 296 297
```

```
    298 299 300 301 302 303 304 305 306 307 308 309 310 311 312 313 314
    315 316 317 318 319 320 321 322 323 324 325 326 327 328 329 330 331
    332 333 334 335 336 337 338 339 340 341 342 343 344 345 346 347 348
    349 350 351 352 353 354 355 356 357 358 359 360 361 362 363 364 365
    366 367 368 369 370 371 372 373 374 375 376 377 378 379 380 381 382
    383 384 385 386 387 388 389 390 391 392 393 394 395 396 397 398 399
    400 401 402 403 404 405 406 407 408 409 410 411 412 413 414 415 416
    417 418 419 420 421 422 423 424 425 426 427 428 429 430 438 439 440
    441 442 443 444 445 446 447 448 449 450 450 451 452 453 454 455 456
    457 458 459 460 461 462 463 464 465 466 467 468 469 470 471 472 473
    474 475 476 477 478 479 480 481 482 483 484 485 486 487 488 489 490
    491 492 493 494 495 496 497 498 499 500 501 502 503 504 505 506 507
    508 509 510 511 512 513 514 515 516 517 518 519 520 521 522 523 524
    525 526 527 528 529 530 531 532 533 534 535 536 537 538 539 540 541
    542 543 544 545 546 547 548 549 550 551 552 553 554 555 556 557 558
    559 560 561 562 563 564 565 566 567 568 569 570 571 572 573 574 575
    576 577 578 579 580 581 582 583 584 585 586 587 588 589 590 591 592
    593 594 595 596 597 598 599 600 601 602 603 604 605 606 607 608 609
    610 611 612 613 614 615 616 617 618 619 620 621 622 623 624 625 626
    627 628 629 630 631 632 633 634 635 636 637 638 639 640 641 642 643
    644 645 646 647 648 649 650 651 652 653 654 655 656 657 658 659 660
    661 662 663 664 665 666 667 668 669 670 671 672 673 674 675 676 677
    678 679 680 681 682 683 684 685 686 687 688 689 690 691 692 693 694
    695 696 697 698 699 700 701 702 703 704 705 706 707 708 709 710 711
    712 713 714 715 716 717 718 719 720 721 722 723 724 725 726 727 728
    729 730 731 732 733 734 735 736 737 738 739 740 741 742 743 744 745
    746 747 748 749 750 751 752 753 754 755 756 757 758 759 760 761 762
    763 764 765 766 767 768 769 770 771 772 773 774 775 776 777 778 779
    780 781 782 783 784 785 786 787 788 789 790 791 792 793 794 795 796
    797 798 799 800 801 802 803 804 805 806 T $Flux Tallies
IMP:p 0 0 0 0 0 0 0 0 0 0 10000 100 100 0 0 0 0 1 0 0 0 0 0 0 0 0 0 0
     0 0 1 100 100 100 100 100 100 100 100 100 100 100 100 500 500 500
     0 0 0 0 0 0 0 0 0 0 0 0 0 0 0 0 0 0 0 0 0 0 0 0 0 0 0 0 0 0 0 0 0 0 0
     0 0 0 0 0 0 0 0 0 0 0 0 0 0 0 0 0 0 0 0 0 0 0 0 0 0 0 0 0 0 0 0 0 0 0
     0 0 0 0 0 0 0 0 0 0 0 0 0 0 0 0 0 0 0 0 0 0 0 0 0 0 0 0 0 0 0 0 0 0 0
     0 0 0 0 0 0 0 0 0 0 0 0 0 0 0 0 0 0 0 0 0 0 1 1 1 1 500 500 500 500
     500 500 500 500 500 500 500 500 500 500 500 500 500 500 500 500 500
     500 500 500 500 500 500 500 500 500 500 500 500 500 500 500 500 500
     500 500 500 500 500 500 500 500 500 500 500 500 500 500 500 500 500
     500 500 500 500 500 500 500 500 500 500 500 500 500 500 500 500 500
     500 500 500 500 500 500 500 500 500 500 500 500 500 500 500 500 500
     500 500 500 500 500 500 500 500 500 500 500 500 500 500 500 500 500
     500 500 500 500 500 500 500 500 500 500 500 500 500 500 500 500 500
     500 500 500 500 500 500 500 500 500 500 500 500 500 500 500 500 500
     500 500 500 500 500 500 500 500 500 500 500 500 500 500 500 500 500
     500 500 500 500 500 500 500 500 500 500 500 500 500 500 500 500 500
     500 500 500 500 500 500 500 500 500 500 500 500 500 500 500 500 500
     500 500 500 500 500 500 500 500 500 500 500 500 500 500 500 500 500
     500 500 500 500 500 500 500 500 500 500 500 500 500 500 500 500 500
     500 500 500 500 500 0 0 100000 0 0 100000 0 500 500 500 500 500 500
     500 500 500 500 500 500 500 500 500 500 500 500 500 500 500 500 500
     500 500 500 500 500 500 500 500 500 500 500 500 500 500 500 500 500
     500 500 500 500 500 500 500 500 500 500 500 500 500 500 500 500 500
     500 500 500 500 500 500 500 500 500 500 500 500 500 500 500 500 500
     500 500 500 500 500 500 500 500 500 500 500 500 500 500 500 500 500
     500 500 500 500 500 500 500 500 500 500 500 500 500 500 500 500 500
     500 500 500 500 500 500 500 500 500 500 500 500 500 500 500 500 500
     500 500 500 500 500 500 500 500 500 500 500 500 500 500 500 500 500
     500 500 500 500 500 500 500 500 500 500 500 500 500 500 500 500 500
     500 500 500 500 500 500 500 500 500 500 500 500 500 500 500 500 500
     500 500 500 500 500 500 500 500 500 500 500 500 500 500 500 500 500
```

```
     500 500 500 500 500 500 500 500 500 500 500 500 500 500 500 500 500
     500 500 500 500 500 500 500 500 500 500 500 500 500 500 500 500 500
     500 500 500 500 500 500 500 500 500 500 500 500 500 500 500 500 500
     500 500 500 500 500 500 500 500 500 500 500 500 500 500 500 500 500
     500 500 500 500 500 500 500 500 500 500 500 500 500 500 500 500 500
     500 500 500 500 500 500 500 500 500 500 500 500 500 500 500 500 500
     500 500 500 500 500 500 500 500 500 500 500 500 500 500 500 500 500
     500 500 500 500 500 500 500 500 500 500 500 500 500 500 500 500 500
     500 500 500 500 500 500 500 500 500 500 500 500 500 500 500 500 500
     500 500 500 500 500 500 500 500 500 500 500 500 500 500 500 500 500
     500 500 500 500 500 500 500
WWP:p 2 1.1 10 0 1 0 1 0
nps   10000000
print
```

B APPENDIX – PARTIAL MCNP5 OUTPUT FOR LOCA SIMULATION; MeV/photon

1tally 8 nps = 10000000
tally type 8* energy deposition units mev
tally for photons

cell 39
7.65668E-06 0.0344
cell 41
7.20878E-06 0.0149
cell 43
6.94475E-06 0.0154
cell 45
6.85553E-06 0.0153
cell 47
6.94157E-06 0.0154
cell 49
6.77631E-06 0.0160
cell 52
6.50256E-06 0.0079
cell 201
1.39436E-10 1.0000
cell 202
7.43429E-09 0.6079
cell 203
4.37828E-10 0.7298
cell 204
1.41857E-08 0.3562
cell 205
1.32356E-09 0.2363
cell 206
-5.03121E-09 0.9964
cell 207
4.78594E-10 0.6603
cell 208
-2.51188E-09 1.0000
cell 209
-1.34325E-10 1.0000
cell 210
8.83095E-09 0.5410
cell 211
4.29245E-10 0.5479
cell 212
3.52819E-09 1.0000
cell 213
6.34917E-10 0.4733
cell 214
3.33833E-08 0.2746
cell 215
4.00725E-10 0.8159
cell 216
2.96418E-08 0.3197
cell 217
-3.53989E-10 0.8462
cell 218
1.96204E-08 0.4699
cell 219

1.64792E-10 1.0000
cell 220
2.07251E-08 0.4031
cell 221
-1.26952E-10 1.0000
cell 222
1.46046E-08 0.5619
cell 223
-2.17286E-11 1.0000
cell 224
3.11102E-08 0.293
cell 225
4.11697E-10 0.6373
cell 226
1.99363E-08 0.4714
cell 227
3.60497E-10 0.8468
cell 228
1.87417E-08 0.4802
cell 229
-1.22580E-10 1.0000
cell 230
6.66424E-09 1.0000
cell 231
-3.99503E-10 0.6044
cell 232
1.99555E-08 0.377
cell 233
-1.28134E-10 1.0000
cell 234
1.11121E-08 0.7485
cell 235
-3.52650E-11 1.0000
cell 236
3.95310E-08 0.2181
cell 237
2.47073E-10 1.0000
cell 238
1.62465E-08 0.5176
cell 239
7.84070E-11 1.0000
cell 240
2.46931E-08 0.3068
cell 241
1.38994E-10 1.0000
cell 242
1.89453E-08 0.3790
cell 243
2.72911E-10 0.8389
cell 244
2.17084E-08 0.3626
cell 245
2.55192E-10 0.9646
cell 246
3.00641E-08 0.2661
cell 247
-1.64902E-10 1.0000
cell 248
1.48509E-08 0.5228
cell 249
3.13994E-10 0.6905

cell 250
2.77053E-08 0.2566
cell 251
4.96144E-10 0.4039
cell 252
1.59292E-08 0.4224
cell 253
6.15501E-11 1.0000
cell 254
3.11376E-08 0.2343
cell 255
4.06298E-10 0.5670
cell 256
2.65631E-08 0.2832
cell 257
2.87032E-10 0.7449
cell 258
2.88546E-08 0.2521
cell 259
6.30261E-10 0.3253
cell 260
1.67573E-08 0.4011
cell 261
2.38478E-10 0.7936
cell 262
1.78655E-08 0.3545
cell 263
4.85098E-10 0.4267
cell 264
3.17767E-08 0.2168
cell 265
2.95688E-10 0.7331
cell 266
3.08311E-08 0.2252
cell 267
5.25865E-10 0.3663
cell 268
1.82452E-08 0.3762
cell 269
2.00140E-10 0.9771
cell 270
2.53563E-08 0.2494
cell 271
3.71482E-10 0.5621
cell 272
3.02393E-08 0.1977
cell 273
4.21626E-10 0.4553
cell 274
2.18579E-08 0.2916
cell 275
3.65036E-10 0.5886
cell 276
2.50815E-08 0.2599
cell 277
5.17164E-10 0.4153
cell 278
3.86343E-08 0.1632
cell 279
5.08859E-10 0.3397
cell 280

2.49583E-08 0.2376
cell 281
4.71245E-10 0.3944
cell 282
2.86224E-08 0.1982
cell 283
2.62623E-10 0.7536
cell 284
2.60212E-08 0.2282
cell 285
3.66666E-10 0.5249
cell 286
3.91958E-08 0.1534
cell 287
2.20130E-10 0.8068
cell 288
2.86248E-08 0.2054
cell 289
4.66464E-10 0.4418
cell 290
2.05945E-08 0.2722
cell 291
6.03475E-10 0.3076
cell 292
2.64717E-08 0.1973
cell 293
7.31498E-10 0.2479
cell 294
2.49366E-08 0.2297
cell 295
3.34122E-10 0.6148
cell 296
3.41430E-08 0.1683

cell 297
4.33002E-10 0.3942

cell 298
3.09322E-08 0.1805

cell 299
6.80865E-10 0.2939
cell 300
3.13115E-08 0.1694
cell 301
4.23048E-10 0.4084
cell 302
3.44367E-08 0.1464
cell 303
5.33460E-10 0.3806
cell 304
4.07613E-08 0.1313
cell 305
3.93170E-10 0.3782
cell 306
3.58571E-08 0.1497
cell 307
2.93220E-10 0.6930
cell 308
2.65651E-08 0.2003
cell 309

3.15720E-10 0.5132
cell 310
2.09667E-08 0.2427
cell 311
5.48451E-10 0.3133
cell 312
2.18636E-08 0.2191
cell 313
1.12008E-10 1.0000
cell 314
3.01675E-08 0.1666
cell 315
3.85597E-10 0.4089
cell 316
3.06600E-08 0.1664
cell 317
5.29915E-10 0.3981
cell 318
3.08015E-08 0.1625
cell 319
3.90866E-10 0.5512
cell 320
3.47770E-08 0.1368
cell 321
4.40564E-10 0.3433
cell 322
3.14917E-08 0.1418
cell 323
5.09665E-10 0.3178
cell 324
2.76440E-08 0.1716
cell 325
3.17765E-10 0.5596
cell 326
2.36935E-08 0.2063
cell 327
5.53683E-10 0.2945
cell 328
2.45148E-08 0.1956
cell 329
4.45389E-10 0.4034
cell 330
1.92757E-08 0.2343
cell 331
5.70171E-10 0.2779
cell 332
2.71441E-08 0.1607
cell 333
5.17316E-10 0.3077
cell 334
3.36814E-08 0.1337
cell 335
5.23937E-10 0.3610
cell 336
4.09290E-08 0.1109
cell 337
3.00546E-10 0.5807
cell 338
2.74646E-08 0.1646
cell 339
5.26832E-10 0.2969

cell 340
2.18903E-08 0.1950
cell 341
6.44296E-10 0.2518
cell 342
2.78755E-08 0.1435
cell 343
4.00803E-10 0.4047
cell 344
2.36723E-08 0.1819
cell 345
4.10131E-10 0.4346
cell 346
2.68172E-08 0.1618
cell 347
8.15785E-10 0.1998
cell 348
2.72027E-08 0.1569
cell 349
4.71551E-10 0.3195
cell 350
3.40523E-08 0.1237
cell 351
3.79162E-10 0.3906
cell 352
2.23201E-08 0.1747
cell 353
5.51137E-10 0.3047
cell 354
1.81807E-08 0.2299
cell 355
7.21411E-10 0.2504
cell 356
2.84168E-08 0.1427
cell 357
3.64570E-10 0.3994
cell 358
2.19861E-08 0.1831
cell 359
4.99784E-10 0.3549
cell 360
2.79302E-08 0.1398
cell 361
1.73851E-10 0.8164
cell 362
2.27267E-08 0.1595
cell 363
7.62197E-10 0.2483
cell 364
2.49520E-08 0.1524
cell 365
7.06170E-10 0.2276
cell 366
2.41437E-08 0.1655
cell 367
4.50114E-10 0.3871
cell 368
2.49065E-08 0.1533
cell 369
1.63259E-10 0.8421
cell 370

2.62744E-08 0.1361
cell 371
4.26180E-10 0.3443
cell 372
3.03354E-08 0.1155
cell 373
4.88497E-10 0.2922
cell 374
1.79180E-08 0.2030
cell 375
6.62358E-10 0.2263
cell 376
2.02818E-08 0.1859
cell 377
5.70792E-10 0.3012
cell 378
2.49213E-08 0.1479
cell 379
3.81853E-10 0.3103
cell 380
1.83853E-08 0.1881
cell 381
5.17216E-10 0.2833
cell 382
2.33239E-08 0.1437
cell 383
5.63549E-10 0.3020
cell 384
2.39616E-08 0.1412
cell 385
5.06513E-10 0.2818
cell 386
2.53259E-08 0.1431
cell 387
5.25647E-10 0.2899
cell 388
2.35554E-08 0.1477
cell 389
3.72290E-10 0.3462
cell 390
2.10901E-08 0.1629
cell 391
3.37702E-10 0.3923
cell 392
1.78592E-08 0.1788
cell 393
5.53965E-10 0.2657
cell 394
2.13407E-08 0.1576
cell 395
4.19981E-10 0.4123
cell 396
2.67075E-08 0.1284
cell 397
3.27337E-10 0.4366
cell 398
2.01932E-08 0.1662
cell 399
5.34532E-10 0.2767
cell 400
1.97695E-08 0.1675

cell 401
6.02781E-10 0.2310
cell 402
2.28384E-08 0.1375
cell 403
5.95663E-10 0.2087
cell 404
2.02565E-08 0.1598
cell 405
6.22775E-10 0.2705
cell 406
2.70167E-08 0.1207
cell 407
6.57629E-10 0.2250
cell 408
1.63788E-08 0.1948
cell 409
7.34062E-10 0.1943
cell 410
2.26593E-08 0.1388
cell 411
6.81059E-10 0.2185
cell 412
2.42449E-08 0.1220
cell 413
8.88776E-10 0.2054
cell 414
2.00070E-08 0.1503
cell 415
5.90913E-10 0.2331
cell 416
2.31146E-08 0.1378
cell 417
6.22989E-10 0.2115
cell 418
2.70306E-08 0.1119
cell 419
4.44982E-10 0.2790
cell 420
2.00573E-08 0.1484
cell 421
9.77778E-10 0.1730
cell 422
2.25826E-08 0.1270
cell 423
1.06418E-09 0.1606
cell 424
2.72843E-08 0.1057
cell 425
6.76644E-10 0.2479
cell 426
2.14776E-08 0.1414
cell 427
6.80986E-10 0.2274
cell 428
1.74603E-08 0.1720
cell 429
7.31419E-10 0.2356
cell 430
1.86567E-08 0.1483
cell 438

7.08223E-10 0.2112
cell 439
2.13237E-08 0.1239
cell 440
7.90651E-10 0.1746
cell 441
1.81075E-08 0.1593
cell 442
8.84656E-10 0.1899
cell 443
2.40281E-08 0.1169
cell 444
7.40936E-10 0.2213
cell 445
2.13231E-08 0.1336
cell 446
7.55079E-10 0.1955
cell 447
1.84425E-08 0.1570
cell 448
1.11674E-09 0.1711
cell 449
1.73093E-08 0.1500
cell 450
9.20481E-10 0.2042
cell 450
9.20481E-10 0.2042
cell 451
2.31642E-08 0.1191
cell 452
4.95095E-10 0.2932
cell 453
2.18239E-08 0.1232
cell 454
9.49303E-10 0.1704
cell 455
2.21819E-08 0.1255
cell 456
5.64355E-10 0.2817
cell 457
2.13288E-08 0.1205
cell 458
7.97755E-10 0.2137
cell 459
1.92886E-08 0.1337
cell 460
1.02097E-09 0.1686
cell 461
1.75823E-08 0.1449
cell 462
1.04479E-09 0.1615
cell 463
2.06673E-08 0.1280
cell 464
7.77093E-10 0.1729
cell 465
2.03200E-08 0.1296
cell 466
6.58274E-10 0.2253
cell 467
1.82007E-08 0.1375

cell 468
7.79825E-10 0.2015
cell 469
2.05365E-08 0.1175
cell 470
8.03849E-10 0.2037
cell 471
1.55842E-08 0.1626
cell 472
9.44060E-10 0.1636
cell 473
2.20907E-08 0.1159
cell 474
1.01090E-09 0.1794
cell 475
1.43933E-08 0.1761
cell 476
8.30673E-10 0.1986
cell 477
1.98894E-08 0.1199
cell 478
5.24943E-10 0.3044
cell 479
1.72725E-08 0.1316
cell 480
9.27430E-10 0.1750
cell 481
1.79732E-08 0.1341
cell 482
1.10684E-09 0.1445
cell 483
1.91239E-08 0.1245
cell 484
1.29129E-09 0.1659
cell 485
1.18077E-08 0.2080
cell 486
7.39617E-10 0.1809
cell 487
1.39640E-08 0.1690
cell 488
8.43592E-10 0.1562
cell 489
1.68490E-08 0.1333
cell 490
1.15181E-09 0.1440
cell 491
1.66543E-08 0.1408
cell 492
8.05403E-10 0.2018
cell 493
1.81519E-08 0.1251
cell 494
9.86328E-10 0.1727
cell 495
1.59628E-08 0.1467
cell 496
8.67984E-10 0.1714
cell 497
1.93092E-08 0.1163
cell 498

7.54682E-10 0.1511
cell 499
1.74509E-08 0.1277
cell 500
7.92763E-10 0.1890
cell 501
1.39295E-08 0.1607
cell 502
1.02142E-09 0.1465
cell 503
1.90288E-08 0.1203
cell 504
6.35929E-10 0.2068
cell 505
2.15095E-08 0.1060
cell 506
8.84261E-10 0.1699
cell 507
1.67079E-08 0.1267
cell 508
7.55150E-10 0.1794
cell 509
1.42038E-08 0.1480
cell 510
8.90660E-10 0.1781
cell 511
1.61881E-08 0.1380
cell 512
8.62736E-10 0.1678
cell 513
1.56059E-08 0.1393
cell 514
9.02816E-10 0.1747
cell 515
1.38195E-08 0.1626
cell 516
6.96170E-10 0.1670
cell 517
1.44118E-08 0.1410
cell 518
7.26930E-10 0.2551
cell 519
1.56775E-08 0.1280
cell 520
9.61808E-10 0.1796
cell 521
1.21332E-08 0.1745
cell 522
9.25841E-10 0.1562
cell 523
1.16918E-08 0.1841
cell 524
8.51887E-10 0.1900
cell 525
1.70039E-08 0.1234
cell 526
7.62229E-10 0.1621
cell 527
1.56861E-08 0.1291
cell 528
8.98189E-10 0.1642

cell 529
1.43090E-08 0.1414
cell 530
9.51558E-10 0.1699
cell 531
1.88472E-08 0.1120
cell 532
7.78272E-10 0.1678
cell 533
1.07235E-08 0.1961
cell 534
1.02457E-09 0.1402
cell 535
1.58944E-08 0.1262
cell 536
8.99720E-10 0.1569
cell 537
1.38238E-08 0.1467
cell 538
6.36126E-10 0.2276
cell 539
1.34439E-08 0.1452
cell 540
6.68212E-10 0.2030
cell 541
1.67256E-08 0.1151
cell 542
7.88191E-10 0.1857
cell 543
1.36371E-08 0.1544
cell 544
6.62737E-10 0.2336
cell 545
1.42224E-08 0.1370
cell 546
4.64221E-10 0.2178
cell 547
1.55049E-08 0.1207
cell 548
8.06071E-10 0.1523
cell 549
1.44246E-08 0.1287
cell 550
8.59650E-10 0.1784
cell 551
1.26581E-08 0.1523
cell 552
7.43287E-10 0.2058
cell 553
1.36345E-08 0.1421
cell 554
7.79828E-10 0.2099
cell 555
1.44581E-08 0.1317
cell 556
8.79618E-10 0.1783
cell 557
1.45399E-08 0.1234
cell 558
1.08477E-09 0.1599
cell 559

1.39787E-08 0.1259
cell 560
5.89350E-10 0.2304
cell 561
1.28092E-08 0.1434
cell 562
6.91486E-10 0.2110
cell 563
1.44584E-08 0.1281
cell 564
1.10275E-09 0.1593
cell 565
1.38554E-08 0.1284
cell 566
8.46758E-10 0.1774
cell 567
1.57341E-08 0.1085
cell 568
7.75807E-10 0.1750
cell 569
1.40725E-08 0.1212
cell 570
6.52302E-10 0.1967
cell 571
1.22076E-08 0.1556
cell 572
7.32381E-10 0.1877
cell 573
1.53713E-08 0.1143
cell 574
7.80395E-10 0.1741
cell 575
1.25113E-08 0.1401
cell 576
8.16916E-10 0.1643
cell 577
1.15516E-08 0.1498
cell 578
7.73654E-10 0.1924
cell 579
1.24350E-08 0.1349
cell 580
7.55429E-10 0.2007
cell 581
1.11300E-08 0.1557
cell 582
6.59694E-10 0.1884
cell 583
1.27181E-08 0.1408
cell 584
9.27730E-10 0.1697
cell 585
1.29916E-08 0.1297
cell 586
9.87082E-10 0.1664
cell 587
7.80577E-09 0.2189
cell 588
5.65924E-10 0.2341
cell 589
1.24594E-08 0.1337

cell 590
8.54663E-10 0.1803
cell 591
1.32080E-08 0.1229
cell 592
4.92758E-10 0.2095
cell 593
1.14348E-08 0.1492
cell 594
9.27093E-10 0.1688
cell 595
1.23719E-08 0.1388
cell 596
5.61888E-10 0.2415
cell 597
1.25301E-08 0.1344
cell 598
7.41553E-10 0.1947
cell 599
1.10944E-08 0.1366
cell 600
8.65163E-10 0.1904
cell 601
1.05522E-08 0.1467
cell 602
5.05926E-10 0.2098
cell 603
1.18343E-08 0.1365
cell 604
7.96386E-10 0.1753
cell 605
1.32279E-08 0.1173
cell 606
8.74903E-10 0.1953
cell 607
1.04828E-08 0.1456
cell 608
8.00202E-10 0.1766
cell 609
1.03478E-08 0.1491
cell 610
7.86642E-10 0.1614
cell 611
1.23510E-08 0.1237
cell 612
9.90682E-10 0.1753
cell 613
9.85168E-09 0.1518
cell 614
7.13463E-10 0.1843
cell 615
1.07146E-08 0.1451
cell 616
7.75236E-10 0.1660
cell 617
1.05903E-08 0.1444
cell 618
7.27202E-10 0.1793
cell 619
9.96684E-09 0.1486
cell 620

5.74758E-10 0.2161
cell 621
1.32310E-08 0.1156
cell 622
7.22335E-10 0.2069
cell 623
8.80790E-09 0.1664
cell 624
5.77762E-10 0.2192
cell 625
7.93121E-09 0.1992
cell 626
9.07384E-10 0.1677
cell 627
1.04652E-08 0.1363
cell 628
7.40472E-10 0.2073
cell 629
7.66968E-09 0.1899
cell 630
7.03279E-10 0.2072
cell 631
9.32334E-09 0.1538
cell 632
9.80308E-10 0.1710
cell 633
8.30312E-09 0.1838
cell 634
6.24311E-10 0.2318
cell 635
9.77802E-09 0.1538
cell 636
6.67116E-10 0.2109
cell 637
8.07438E-09 0.1715
cell 638
6.68797E-10 0.1968
cell 639
9.41005E-09 0.1489
cell 640
6.72500E-10 0.2213
cell 641
9.76102E-09 0.1477
cell 642
4.84783E-10 0.2258
cell 643
8.12015E-09 0.1835
cell 644
6.72798E-10 0.2101
cell 645
8.87657E-09 0.1606
cell 646
7.45770E-10 0.1766
cell 647
8.87777E-09 0.1591
cell 648
3.32277E-10 0.2810
cell 649
7.15869E-09 0.1839
cell 650
5.37529E-10 0.2356

cell 651
9.53157E-09 0.1447
cell 652
3.92599E-10 0.2183
cell 653
9.50066E-09 0.1484
cell 654
4.11897E-10 0.3049
cell 655
1.05954E-08 0.1295
cell 656
4.94158E-10 0.2320
cell 657
8.81547E-09 0.1648
cell 658
7.97754E-10 0.1910
cell 659
6.65305E-09 0.2055
cell 660
6.00458E-10 0.1793
cell 661
8.56252E-09 0.1500
cell 662
6.54928E-10 0.1975
cell 663
6.89169E-09 0.2010
cell 664
6.11663E-10 0.2267
cell 665
8.29812E-09 0.1618
cell 666
5.28714E-10 0.2328
cell 667
5.82713E-09 0.2272
cell 668
3.97955E-10 0.3032
cell 669
8.84000E-09 0.1415
cell 670
5.23429E-10 0.2390
cell 671
6.84141E-09 0.1941
cell 672
6.29799E-10 0.1892
cell 673
9.12697E-09 0.1385
cell 674
6.54125E-10 0.1824
cell 675
1.17401E-08 0.1119
cell 676
5.46896E-10 0.1912
cell 677
8.18843E-09 0.1563
cell 678
4.46247E-10 0.2812
cell 679
7.66660E-09 0.1596
cell 680
3.29531E-10 0.2952
cell 681

9.47374E-09 0.1326
cell 682
4.73623E-10 0.2862
cell 683
8.11371E-09 0.1603
cell 684
3.93345E-10 0.2151
cell 685
7.72110E-09 0.1658
cell 686
6.05003E-10 0.1998
cell 687
7.00840E-09 0.1765
cell 688
7.14497E-10 0.1951
cell 689
5.93416E-09 0.2015
cell 690
5.81057E-10 0.2043
cell 691
7.02645E-09 0.1795
cell 692
5.02666E-10 0.2099
cell 693
8.67333E-09 0.1436
cell 694
4.72129E-10 0.2680
cell 695
6.17618E-09 0.1958
cell 696
7.16153E-10 0.1838
cell 697
8.42865E-09 0.1316
cell 698
5.35164E-10 0.2157
cell 699
7.15759E-09 0.1623
cell 700
5.36793E-10 0.231
cell 701
7.93359E-09 0.1577
cell 702
7.02212E-10 0.2039
cell 703
7.65027E-09 0.1647
cell 704
5.31447E-10 0.2246
cell 705
8.36032E-09 0.1438
cell 706
6.70411E-10 0.2056
cell 707
5.53061E-09 0.2155
cell 708
3.48549E-10 0.2818
cell 709
7.19610E-09 0.1504
cell 710
5.59455E-10 0.2667
cell 711
6.65557E-09 0.1929

cell 712
4.78059E-10 0.2483
cell 713
6.38878E-09 0.1949
cell 714
6.50670E-10 0.2075
cell 715
7.93112E-09 0.1438
cell 716
4.44894E-10 0.2113
cell 717
9.50360E-09 0.1198
cell 718
6.95859E-10 0.1970
cell 719
7.48404E-09 0.1458
cell 720
5.47400E-10 0.2324
cell 721
6.54259E-09 0.1784
cell 722
7.77193E-10 0.1960
cell 723
6.10067E-09 0.1911
cell 724
4.01634E-10 0.2855
cell 725
5.66136E-09 0.2089
cell 726
5.38918E-10 0.2634
cell 727
6.44297E-09 0.1719
cell 728
4.25422E-10 0.2214
cell 729
5.41678E-09 0.2071
cell 730
4.39279E-10 0.2767
cell 731
5.82279E-09 0.1867
cell 732
6.68677E-10 0.2177
cell 733
7.35046E-09 0.1569
cell 734
3.94183E-10 0.2554
cell 735
7.24313E-09 0.1487
cell 736
4.15704E-10 0.2626
cell 737
6.02337E-09 0.1747
cell 738
4.47315E-10 0.2347
cell 739
6.30593E-09 0.1664
cell 740
6.35865E-10 0.2000
cell 741
5.28617E-09 0.2017
cell 742

4.52986E-10 0.2736
cell 743
4.20163E-09 0.2631
cell 744
6.28359E-10 0.2007
cell 745
5.60780E-09 0.1898
cell 746
3.26352E-10 0.2494
cell 747
6.12360E-09 0.1740
cell 748
4.26777E-10 0.2377
cell 749
5.91607E-09 0.1748
cell 750
5.15301E-10 0.2443
cell 751
4.70864E-09 0.2322
cell 752
6.22603E-10 0.2255
cell 753
4.45476E-09 0.2410
cell 754
2.96114E-10 0.2946
cell 755
4.98047E-09 0.2133
cell 756
4.48265E-10 0.2198
cell 757
5.03954E-09 0.2109
cell 758
3.80949E-10 0.2977
cell 759
6.86266E-09 0.1464
cell 760
3.64861E-10 0.3056
cell 761
5.28300E-09 0.1897
cell 762
3.08014E-10 0.3452
cell 763
6.75919E-09 0.1553
cell 764
4.93430E-10 0.2537
cell 765
4.04862E-09 0.2729
cell 766
3.22790E-10 0.3853
cell 767
4.19753E-09 0.2494
cell 768
4.28499E-10 0.2548
cell 769
5.70221E-09 0.1821
cell 770
3.05005E-10 0.3255
cell 771
5.89340E-09 0.1719
cell 772
3.94530E-10 0.2597

cell 773
5.09008E-09 0.2053
cell 774
5.93871E-10 0.2040
cell 775
6.96450E-09 0.1443
cell 776
2.97756E-10 0.3136
cell 777
6.60038E-09 0.1447
cell 778
3.22503E-10 0.2678
cell 779
6.53242E-09 0.1491
cell 780
3.38165E-10 0.2819
cell 781
5.35633E-09 0.1806
cell 782
3.54633E-10 0.3326
cell 783
4.91355E-09 0.2156
cell 784
3.72854E-10 0.2474
cell 785
3.84998E-09 0.2465
cell 786
5.58339E-10 0.2325
cell 787
5.83208E-09 0.1506
cell 788
2.19362E-10 0.2895
cell 789
3.98979E-09 0.2227
cell 790
3.70666E-10 0.2703
cell 791
5.27244E-09 0.1802
cell 792
4.60945E-10 0.2700
cell 793
4.29081E-09 0.2227
cell 794
4.60978E-10 0.2269
cell 795
6.05145E-09 0.1578
cell 796
3.69119E-10 0.2465
cell 797
3.29916E-09 0.2873
cell 798
4.24792E-10 0.2768
cell 799
4.02106E-09 0.2412
cell 800
2.30036E-10 0.3017
cell 801
5.66442E-09 0.1758
cell 802
3.66076E-10 0.3028
cell 803

5.13792E-09 0.1751
cell 804
4.78647E-10 0.2140
cell 805
3.72178E-09 0.2416
cell 806
7.07048E-10 0.1989
cell union total
5.38516E-05 0.0071